Co-option of local and systemic immune responses by the hormonal signalling system triggering metamorphosis in *Drosophila melanogaster*

Catarina Nunes[1*], Takashi Koyama[2], Élio Sucena[1,3*]

[1] Evolution and Development Laboratory, Instituto Gulbenkian de Ciência, Oeiras, Portugal

[2] Section for Cell and Neurobiology, Department of Biology University of Copenhagen, Copenhagen, Denmark

[3] Departamento de Biologia Animal, Faculdade de Ciências, Universidade de Lisboa, Lisbon, Portugal

* Corresponding author

Email: cdnunes@igc.gulbenkian.pt (CN)

esucena@igc.gulbenkian.pt (ES)

Abstract

Insect metamorphosis is regulated by the production, secretion and degradation of two peripheral hormones: 20-hydroxyecdysone (ecdysone) and juvenile hormone (JH). In addition to their roles in developmental regulation, increasing evidence suggests that these hormones are involved in innate immunity processes, such as phagocytosis and the induction of antimicrobial peptide (AMP) production. AMP regulation includes systemic responses and local responses, at surface epithelia that contact with the external environments. At pupariation, *Drosophila melanogaster* increases dramatically the expression of three AMP genes: *drosomycin (drs)*, *drosomycin-like 2 (drsl2)* and *drosomycin-like 5 (drsl5)*. Using *D. melanogaster,* we show that the expression of *drs* at pupariation is dependent on ecdysone signalling in the fat body. This systemic immune response involving *drs* expression in the fat body operates via the ecdysone downstream target, Broad-Z4. In parallel, ecdysone also regulates local responses, specifically through the activation of *drsl2* expression in the gut. Finally, we establish the relevance of this ecdysone dependent AMP expression for the control of bacterial persistence by showing that flies lacking *drs* expression in the fat body have higher bacterial persistence over metamorphosis. Together, our data emphasize the importance of the association between ecdysone signalling and immunity using *in vivo* studies and establishes a new role for ecdysone at pupariation. This co-option of immune mechanisms by the hormonal cascade responsible for controlling metamorphosis impact developmental success by regulating the immune system in a stage-dependent manner. We speculate it may constitute a pre-emptive mechanism to control bacterial numbers in the pupa at the core of metamorphosis evolution.

Introduction

Insect development and physiology are mainly regulated by two peripheral hormones: the steroid hormone, 20-hydroxyecdsyone (hereafter, ecdysone) and the sesquiterpenoid hormone, juvenile hormone (JH) [1,2]. In vertebrates, steroid hormones and their nuclear receptors are key

regulators of systemic immune responses, namely through the enhancement of inflammation [3]. Similarly, in insects, steroid hormones are also known to be involved in innate immunity [4–9]. In insects, ecdysone titre is tightly regulated during development and as such, steroid hormone-dependent activation of innate immunity seems appropriate for stage-specific regulation of immunity.

When in contact with a microorganism, insects rely on the activation of three tightly related immunity processes: i) cellular immunity (i.e. phagocytosis and encapsulation of invading microorganisms); ii) the induction of proteolytic cascades, that culminate in melanisation; and iii) production of antimicrobial peptides (AMPs), which is primarily regulated at the transcriptional level through two distinct signalling pathways, Toll and Imd, triggered by sensing of Lys-type peptidoglycan and β-1,3-glucan or meso-diaminopimelic acid (DAP)-type peptidoglycan, respectively [10–12]. In insects with complete metamorphosis (holometabolans), AMP genes are usually silent in the absence of an immune challenge and their expression is induced upon injury and/or infection [13]. However, indirect evidence suggests that AMPs may be up-regulated at specific developmental stages irrespective of pathogen presence. Studies in the moth *Manduca sexta* show that expression of lysozyme and of the AMPs *cecropin A*, *cecropin B* and *hemolin* increases dramatically during metamorphosis, although it is not clear what regulates this increase [14–16]. This transcriptional AMP peak occurs before the end of histolysis of the larval midgut, that is, before cells are potentially exposed to any pathogen or bacterium. In this context, the accumulation of AMPs at the end of the feeding stage may constitute a response against the possible harmful effects inside the pupal body of bacteria carried-over from the gut remodelling process, although there is no definite evidence for this claim [17–20]. Nonetheless, studies in dipterans show that some species of bacteria can persist inside the host throughout metamorphosis from the larval guts [19–22]. In *Drosophila melanogaster,* up-regulation of several *drosomycin* (*drs*) paralogues has also been reported at pupariation [23]. Furthermore, five different AMPs (*diptericin, drs, attacin-A, metchnikowin* and *cecropin A1*) are shown to contain putative *cis*-regulatory elements for potential binding of the functional ecdysone receptor complex, suggesting

77 an ecdysone-dependent control of their expression [24]. Importantly, the compelling association
78 between ecdysone signalling and immunity at this particular stage of development is not restricted
79 to the humoral arm of the immune response. An ecdysone-dependent increase in phagocytic
80 capacity of plasmatocytes at pupariation has been described and hypothesized to be particularly
81 important given the higher predisposition for infection at the pupal stage [6].

82 In *D. melanogaster*, RNAseq analysis revealed a peak in the expression of AMPs at
83 pupariation, of which around 95% consists of three AMPs: *drs*, *drosomycin-like 2 (drsl2)* and
84 *drosomycin-like 5 (drsl5)* (S1 Fig**,** [23]). Considering the temporal coincidence between this
85 phenomenon and the ecdysone peak at pupariation to regulate metamorphosis, we hypothesized
86 that ecdysone signalling controlling development was co-opted to regulate the expression of
87 AMPs at pupariation as a pre-emptive mechanism to control bacterial proliferation and prevent
88 possible infections during metamorphosis associated with the gut reconstruction. Previous *in vitro*
89 study has shown that ecdysone promotes humoral immunity by increasing the expression of AMP
90 genes, such as *diptericin, cecropin* and *attacin,* via the EcR-USP receptor complex in S2 cells [5].
91 In addition, a microarray analysis of 20E-treated S2 cells revealed the existence of two distinct
92 mechanisms for 20E-regulated AMP expression: one in which the critical step is the activation of
93 peptidoglycan recognition protein (PGRP)-LC - a critical pattern recognition receptor (PRR) of
94 the Imd pathway - by ecdysone for controlling the expression of *cecropin A1, attacin-A and*
95 *defensin*; and another, in which the hormonally-controlled mechanism is absolutely required for
96 the expression of *drs, metchnikowin* and *diptericin* [4]. However, the importance of the
97 requirement of ecdysone for the expression of AMPs has not been explored and the regulatory
98 mechanism through which this hormone affects innate immunity remains to be explored.

99 In this study, we demonstrate that ecdysone regulates the expression of AMPs *in vivo* at
100 pupariation, both systemically (by regulating the expression of *drs*) and locally in the midgut (by
101 regulating the expression of *drsl2*). Importantly, the systemic expression of *drs* has an impact on
102 the number of bacteria that persists and proliferates during metamorphosis, corroborating the
103 hypothesis that the AMP peak has a function in controlling bacteria during metamorphosis.

104 Furthermore, we show that this association between the expression of *drs* and ecdysone in the
105 absence of infection occurs solely at pupariation and through the early ecdysone-response gene
106 Broad-Z4, which is only expressed at the end of the feeding stage [25]. Taken together, our
107 findings fill a gap in current knowledge by shedding light onto the mechanisms and biological
108 significance of hormonal control of humoral immunity at metamorphosis with potential
109 evolutionary importance.

Results

drs, drsl2 and *drsl5* are expressed at pupariation in a bacteria-independent manner

Around 95% of the AMP peak at pupariation consists of three AMPs: *drs, drsl2* and *drsl5*. Due to the gut remodelling at metamorphosis, an ineffective gut purge could lead to the activation of the canonical immunity pathways, resulting in an AMP peak. To test this, we determined the expression of *drs, drsl2* and *drsl5* in mid-L3 larvae (L3) and newly pupariated (P0) samples of germ-free (GF) or standardly-raised individuals by quantitative PCR (qPCR). We confirmed that expression increases at pupariation for all AMPs tested (Fig 1 (A), S2 Fig), including *drs (lsmean, pairwise~{w-};+;+ | Stage*drs<0.0001), drsl2 (lsmeans(pairwise~{w};+;+|Stage*drsl2 <0.0001))* and *drsl5 (lsmeans(pairwise~{w-};+;+|Stage*drsl5<0.000))*. This increment is not lost under GF conditions with the putative exceptions of *cecropinA1* and *defensin*. Importantly, the three main AMPs under scrutiny, *drs, drsl2* and *drsl5*, show a marked independence of the presence of microbes (including yeast) for their expression at this developmental transition (*lsmeans(pairwise~{w};+;+|Stage*drs <0.0001); lsmeans(pairwise~{w-}; +;+|Stage*drsl2<0.0001); lsmeans(pairwise~{w};+;+|Stage*drsl5 <0.0001))* (Fig 1 (A), S1 Table).

Together, these results reject the hypothesis that the AMPs expression at pupariation is dependent on microbial induction and suggest that it may be hard-wired to the developmental programme.

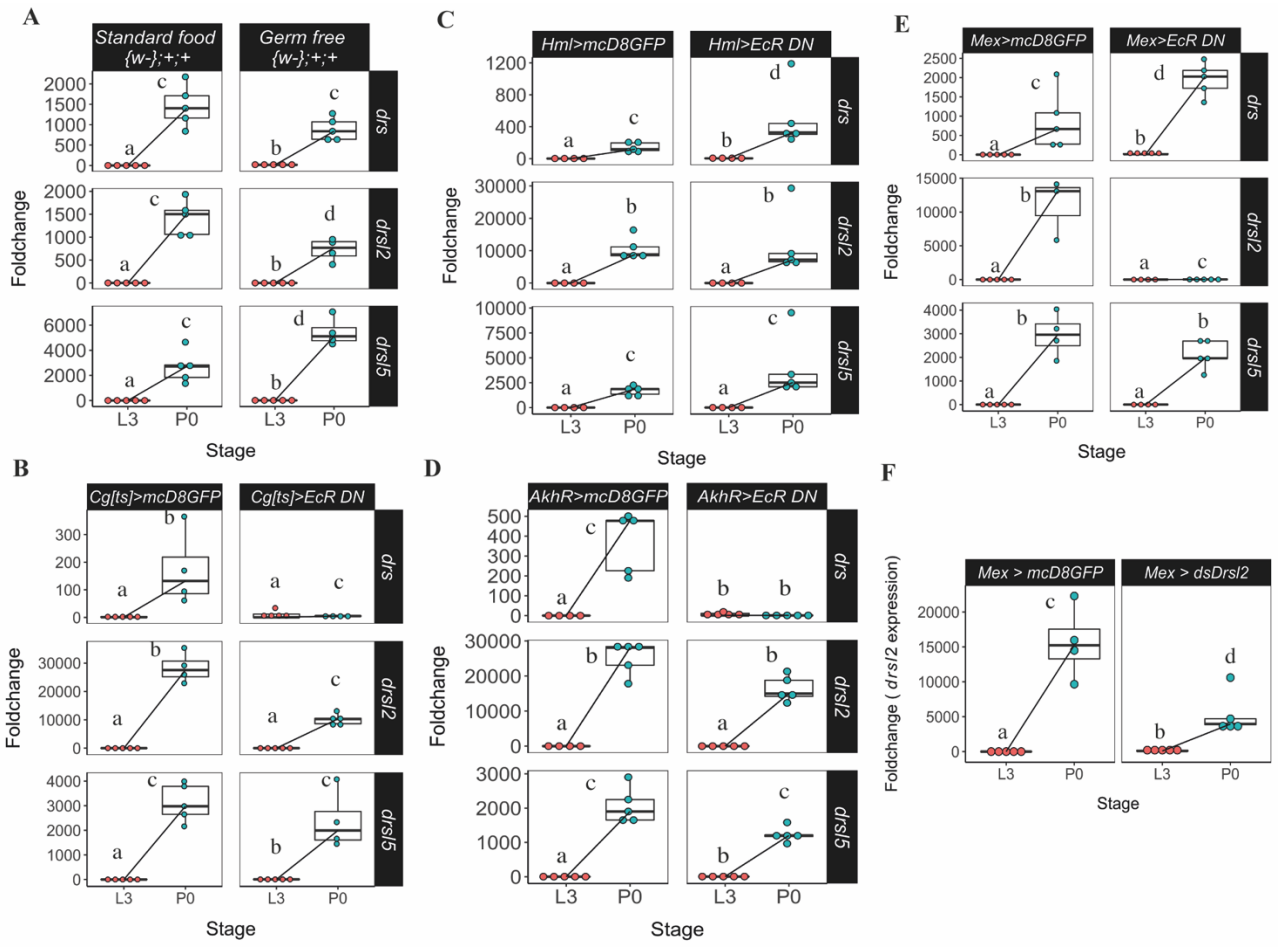

Fig 1. Expression of AMPs at pupariation is developmentally regulated by ecdysone in the fat body. (A) The expression levels of *drs*, *drsl2* and *drsl5* increase at pupariation and are not lost in GF conditions. **(B)** Foldchange increase in *drs* expression (but not of *drsl2* or *drsl5*) at pupariation was eliminated when ecdysone sensitivity is decreased specifically in the fat body and haemocytes simultaneously. **(C)** Reduced ecdysone sensitivity in the haemocytes does not affect the expression of the AMPs under study. (**D**) Reduced ecdysone signalling in the fat body resulted in decreased *drs* expression at pupariation (*lsmeans(pairwise~Stage|AkhR>mcD8GFP <0.0001, lsmeans(pairwise~Stage|AkhR>EcR DN)=0.6709*), without affecting the expression of *drsl2* and *drsl5* (*lsmeans (pairwise~Stage|AkhR>mcD8GFP)<0.0001*, *lsmeans(pairwise~Stage|AkhR>EcRDN)<0.0001)*, for both genes). **(E)** Manipulation of ecdysone sensitivity specifically in the midgut reduced the expression of *drsl2*, but not of *drs* or *drsl5*. **(F)** Knock-down of *drsl2* specifically in the midgut resulted in an overall decrease in the expression of this AMP. Each dot represents a sample of five pooled individuals; the lines connect the median of the samples at L3 and P0; different letters represent statistically significant differences in foldchange. Foldchange was determined using the ΔΔCT method.

Ecdysone regulates the systemic expression of *drs*

We focused primarily on two main sources of systemic AMP expression, the fat body and haemocytes. We manipulated ecdysone signalling sensitivity in these tissues, simultaneously and specifically, to ensure no perturbation of normal development and pupariation timing. For that we used *Cg-Gal4* combined with a *tub-Gal80[ts]*, a thermo-sensitive allele of *Gal80* under the control of the tubulin promoter (hereafter *Cg[ts]*), to drive the expression of a dominant negative ecdysone receptor under the control of the UAS sequence [26] *(EcR-A DN W650A TP3*, hereafter *EcRDN*). The reduction of ecdysone sensitivity was triggered from the onset of L3 or at wandering stage, resulting in elimination of *drs* peak at P0, compared to control conditions (Fig 1 (B), (*lsmeans(pairwise~Stage|Cg[ts]>mcD8GFP)=0.0001*, lsmeans(pairwise~Stage|*Cg[ts]>EcRDN)* =0.0017, lsmeans(pairwise~Genotype|P0)<0.0001)). However, the expression of *drsl2* and *drsl5* (Fig 1 (B), S2 Table) and of the other AMPs (S2 Fig, S2 Table) were not eliminated. Furthermore, *drs* expression still increases in mutant flies for *dif,* the NF-κB factor that triggers *drs* expression upon activation of the Toll pathway (S2 Fig, lsmeans(pairwise~Stage|*{w-};+;+*<0.0001, *lsmeans(pairwise~Stage|{w-};dif1;+)*<0.0001, *lsmeans(pairwise~Genotype|P0)= 0.0703*)), suggesting that the expression of *drs* at pupariation is partially independent of the action of the NF-κB factor.

This was further confirmed by targeting haemocytes and fat body independently, using *Hemolectin-Gal4* (*Hml-ΔGal4*) for the haemocytes and *Adipokinetic hormone receptor-Gal4* (*AkhR-Gal4)* for the fat body. When ecdysone sensitivity was reduced in the haemocytes but not in the fat body, expression of *drs*, *drsl2* and *drsl5,* as well as of other 4 AMPs, was unaffected (*lsmeans(pairwise~Stage|Hml>mcD8GFP)<0.0001*, *lsmeans(pairwise~Stage|Hml>EcR DN)<0.0001*), for the three genes), (Fig 1 (C) and S3 Fig, S3 Table). However, although reduced ecdysone sensitivity in the fat body (*AkhR>EcRDN*) did not affect the expression of *drsl2* and *drsl5* (Fig 1 (D), (*lsmeans(pairwise~Stage|AkhR>mcD8GFP)<0.0001*, *lsmeans (pairwise~Stage|AkhR>EcRDN)<0.0001),* for both genes)) or of other AMPs (S3 Fig, S4 Table),

170 it resulted in decreased expression of *drs* at pupariation. (Fig 1 (D),
171 *lsmeans(pairwise~Stage|AkhR>mcD8GFP)<0.0001, lsmeans(pairwise~Stage|AkhR>EcR DN)*
172 *=0.6709*)).
173 Altogether, these results indicate that *drs* expression - but not *drsl2* or *drsl5* - is systemically
174 regulated by ecdysone signalling specifically in the fat body at pupariation.

175 Local expression of *drsl2* in the midgut is regulated by
176 Ecdysone

177 Having determined that the expression of these other AMPs, particularly *drsl2* and *drsl5*,
178 are developmentally regulated, but not in the fat body, we turned our attention to two of the most
179 important tissues for local immune response: the epithelial layers of the gut and trachea. First, we
180 overexpressed *EcRDN* specifically in the most abundant cells of the midgut, the enterocytes
181 (*Mex>EcRDN*). Unlike the fat body, the gut is not responding to the pupariation ecdysone pulse by
182 increasing *drs* expression (Fig 1 (E)). In contrast, decreased ecdysone sensitivity specifically in
183 the midgut resulted in a drastic reduction (*circa* 600-fold) of *drsl2* expression, very close to the L3
184 basal levels (Fig 1 (E), *lsmeans(pairwise~Genotype|P0)<0.0001; lsmeans(pairwise~Stage|Mex>*
185 *EcRDN) <0.0001*)). Moreover, knock-down of *drsl2* specifically in the midgut (*MexGal4>ds-*
186 *drsl2*) resulted in an overall decrease in the expression of this AMP at pupariation (Fig 1 (F),
187 *lsmeans(pairwise~Genotype|P0)<0.0237; lsmeans(pairwise~Stage|Mex>ds-drsl2) <0.0001*)),
188 which indicates that the midgut is the main source for the ecdysone-dependent production of *drsl2*
189 at this stage. Other tested AMPs also appear to be, at least partially, regulated by ecdysone
190 signalling in the midgut. Under ecdysone-signalling down-regulation conditions, significant
191 decrease in mRNA levels were observed for: *cecropin A1*
192 (*lsmeans(pairwise~Genotype|P0)<0.0001; lsmeans(pairwise~Stage|Mex>EcRDN)=0.0038),*
193 *defensin (lsmeans (pairwise~Genotype|P0)<0.0001; lsmeans(pairwise~Stage|Mex>EcR*
194 *DN)=0.3866*), *metchnikowin* (*lsmeans(pairwise~Genotype|P0)=0.0060; lsmeans*

195 *(pairwise~Stage|Mex>EcRDN<0.0001)*, and *drsl3 ((lsmeans(pairwise~Genotype|P0)=0.0008;*
196 *lsmeans(pairwise~Stage|Mex>EcRDN)= 0.2084*), S3 Fig). Interestingly, no difference was
197 detected in the expression of *drsl5*, one of the three main players in the AMP peak (Fig 1 (E),
198 *lsmeans (pairwise~Genotype|P0)<0.4479; lsmeans(pairwise~Stage|Mex>EcRDN)<0.0001*)).
199 In contrast, decreased ecdysone sensitivity in the trachea (*btl>EcRDN*) did not have an impact on
200 the expression of any of the three major AMPs under study (S3 Fig, S6 Table).
201 Together, these results show that the local sensing of the ecdysone peak at the onset of pupariation
202 in, at least the gut epithelium, controls the production of AMPs. The local and systemic
203 mechanisms that share ecdysone control account for the expression of the genes that constitute
204 about 70% of the pupariation AMP peak. Furthermore, the data also point towards an alternative
205 mechanism for regulating the expression of *drsl5* at pupariation, which is either independent of
206 ecdysone or is regulated by this hormone in an alternative tissue or cell type that were not tested.

207 Systemic expression of *drs* is necessary to reduce bacteria 208 derived from imperfect larval gut purge

209 Before pupariation, larvae purge their gut contents to undergo metamorphosis. Any
210 imperfection in this process creates the conditions in the pupa for a putatively rampant infection.
211 Thus, we examined whether or not gut purge eliminates all bacteria from the gut. Under our
212 standard rearing conditions, the mortality between P0 and pharate adult is negligible, which allows
213 us to infer and correlate the bacterial numbers detected in each of these developmental stages (S4
214 Fig, S7 Table).
215 After gut purge, approximately 5% of control P0 individuals contained bacteria in the
216 order of the thousands and another 12% in the order of the hundreds (Fig 2 (A)). However, at the
217 pharate adult stage, these two classes decreased in number alongside an increase in the number of
218 individuals without detectable bacteria (Fig 2 (B)). In contrast, *drs* null mutants showed an
219 increase rather than a decrease in the number of pupae with more bacteria between these two

220 stages (Fig 2 (C) and (D)), supporting that Drs is necessary to eliminate gut derived bacteria
221 during metamorphosis.
222 Using a resampling strategy, we determined that most coefficients associated with the
223 control line were negative (Fig 2 (G) (*Median: -2.279 (IQR: -2.682 -1.803); One-way Wilcoxon*
224 *test for median<0: <2.2e-16, r= 0.864)* and Fig 2 (I) *(Median: -2.317 (IQR: -2.907 -1.858); One-*
225 *way Wilcoxon test for median<0: <2.2e-16, r=0.866)*). In contrast, the coefficients associated
226 with *drs* null mutant were mostly positive for both bacteria types (Fig 2 (H) *((Median: 0.596*
227 *(IQR: 0.359; 0.757); One-way Wilcoxon test for median> 0: <2.2e-16, r= 0.845*) and Fig 2 (J)
228 (*Median: 2.055 (IQR: 1.897; 2.192); One-way Wilcoxon test for median> 0: <2.2e-16, r=0.866*)).
229 These results suggest that pupae have the bacteria eliminated in a process that is dependent on an
230 increase of AMPs expression at pupariation. This process is necessary for controlling the
231 persistence of bacteria originating from gut purge imperfections, throughout metamorphosis.
232 When ecdysone signalling activity is decreased in the fat body and haemocytes, a similar pattern
233 can be observed: there is a higher proportion of individuals with larger loads of persisting bacteria
234 (Fig 2 (E-F)). The resampling strategy revealed that *Cg[ts]>EcR DN* samples have positive slope
235 values for both *Lactobacillus* (Fig 2 (K), *Median: 2.746 (IQR: 2.562; 2.930); One-way Wilcoxon*
236 *test for median>0: <2.2e-16, r=0.866)* and *Acetobacter* (Fig 2 (L), *Median: 1.981 (IQR: 1.795;*
237 *2.184); One-way Wilcoxon test for median>0: <2.2e-16, r=0.866)*, which is in accordance with
238 increased bacterial loads during metamorphosis. Importantly, *Mex>EcRDN* individuals do not
239 have increased bacterial loads during metamorphosis, suggesting that the local immune response
240 does not have a measurable antibacterial effect relatively to the systemic response that is still
241 operating in these conditions (S3 Fig). In fact, this is in accordance to previous studies that fail to
242 associate an antibacterial activity to Drsl peptides [27]. However, these AMPs are expressed upon

243 *Erwinia carotovora* infection, which suggests that they may be relevant during an immune

244 challenge [27].

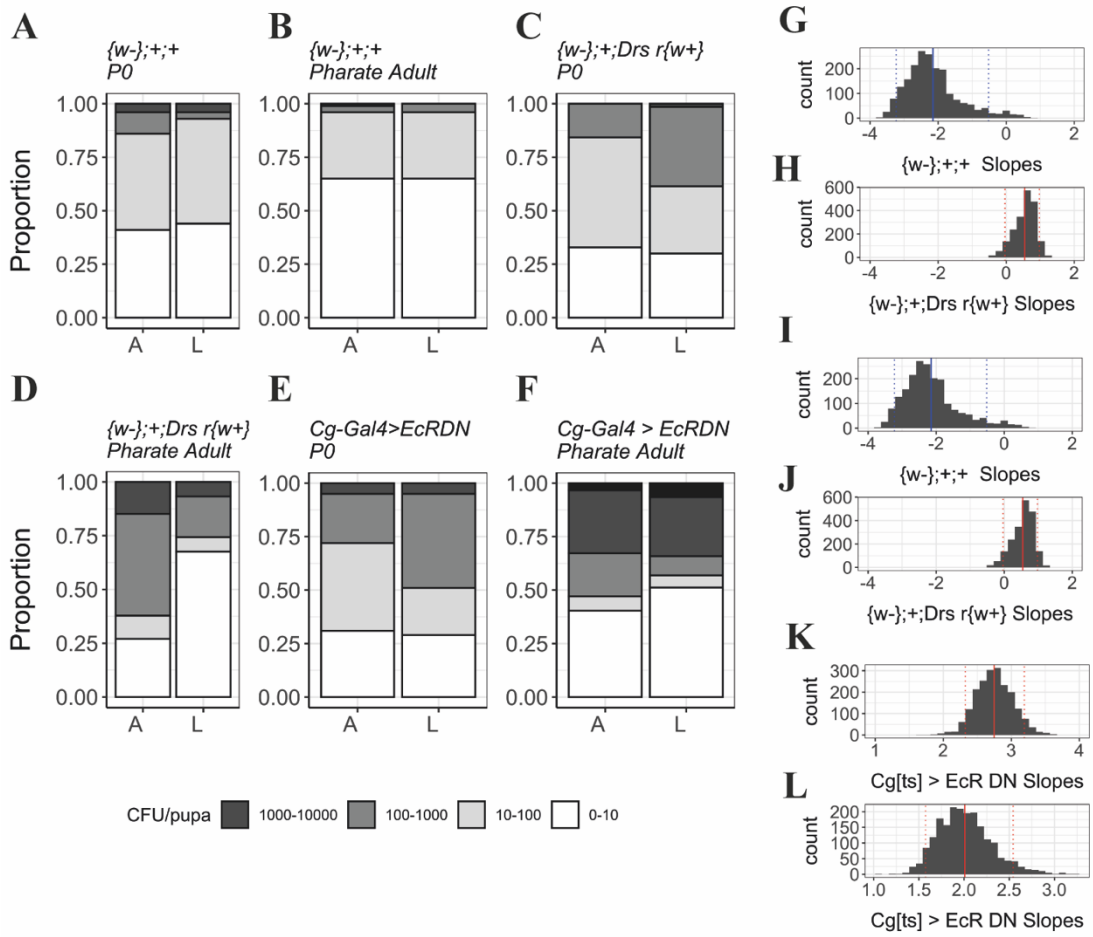

245

246 **Fig 2. (A-F)** Quantification in P0 pupae and pharate adults of *Lactobacillus* (L), growing in selective

247 MRS medium, and *Acetobacter* (A), growing on selective D-Mannitol. **(A-B)** In control flies ({*w-*

248 *};+;+*)**,** the number of pupae with more bacteria decreases between P0 and pharate adult stages. **(C-D)**

249 In the *drs* mutant line ({*w-};+; Drs r{w+}*), there are more individuals with higher loads of bacteria

250 persisting from P0 to pharate adult. **(E-F)** When ecdysone sensitivity is decreased in fat body and

251 haemocytes, the number of both bacteria types increases in P0 and pharate adults. Y-axis represents the

252 proportion of individuals in each bacterial count category. **(G-H)** Slopes for the number of

253 *Lactobacillus* in control and the mutant lines. **(G)** Control samples have negative slopes, representative

254 of a decrease in the number of bacteria between stages. **(H)** *drs* mutant samples have positive slope

255 values, representative of an increase in the number of bacteria between the stages. **(I-J)** Slopes for the

256 number of *Acetobacter* in the control and the mutant lines. **(I)** Control samples distribution show

negative slopes, i.e., a decrease in the number of bacteria between stages. **(J)** *drs* null mutant showed a positive slope values. **(K-L)** Coefficient (slopes) distribution in *Cg[ts]>EcRDN* samples of *Lactobacillus* (**K**) and *Acetobacter***.** Doted lines represent the 0.05 and 0.95 quantiles; full line represents the mean slope**.**

Br is involved in systemic *drs* induction through the fat body at pupariation

Our evidence suggests that the systemic expression of *drs* is more important than the local production of AMPs for the control of bacterial persistence during metamorphosis. Hence, we focused our efforts in trying to uncover the molecular regulation of temporal *drs* expression. Previous RNAseq data showed that the expression of *drs* markedly increases at pupariation (S1 Fig, [23]). We further confirmed that the expression of *dhr3* (a gene directly regulated by the ecdysone-ecdysone receptor complex) and that of *drs* are tightly correlated and peak exclusively at pupariation (S5 Fig). Importantly, this robust expression of *drs* at the onset of metamorphosis seems to be a general feature regardless of their genetic background (S5 Fig).

br is a direct target of ecdysone receptor, characterized as a holometabolan pupal specifier with increased expression before pupariation [25,28,29]. We examined the association between *br* and the ecdysone-sensitive systemic induction of *drs* at metamorphosis by knocking-down *br* specifically in the fat body and haemocytes. This led to a significant decrease in the expression of *drs* at pupariation, when compared to the control (Fig 3 (A), *lsmeans(pairwise~Genotype|P0)= 0.0510*)), suggesting a role for *br* in the regulation of AMP expression. To further explore this possibility, we simultaneously reduced ecdysone signalling and restored *br* in the haemocytes and fat body. This was sufficient to rescue the expression of *drs* to control levels at P0 (Fig 3 (B), *lsmeans(pairwise~Genotype|P0)= 0.3068*). Furthermore, we generated two different conditional CRISPR-mediated knock-out constructs [30,31], one targeting a common region to all *br* isoforms and, the other, a region specific to *br-Z4,* previously associated with AMP expression in a

282 different species [32]. Knock-out of all *br* isoforms or of *br-Z4* alone in haemocytes and fat body,
283 led to the elimination of the *drs* peak at pupariation (Fig 3 (C), *lsmeans(pairwise~Stage|Cg>*
284 *+;Cas9;+) <0.0001;lsmeans(pairwise~Stage| Cg>Cas9;br KO)=0.0001,*
285 *lsmeans(pairwise~Stage|Cg>Cas9;br-Z4 KO)=0.4691*), supporting that Br is involved in the
286 regulation of *drs* expression at pupariation downstream of the ecdysone receptor complex.
287 To further explore this regulation of *drs* expression by Br-Z4, we used the JASPAR
288 (http://jaspar.genereg.net) matrix MA0013.1 to run a comprehensive search for Br-Z4 binding
289 sites over 2 kb of putative promoter region that is upstream of the coding sequence of *drs*,
290 obtained from Flybase (http://flybase.net/), using FIMO software [33] (S5 Fig). We identified

291 three putative Br-Z4 binding sites (p-value<0.0001) in the predicted 5' promoter region of *drs* (S5
292 Fig (D)).
293 Together, these results support the idea that Br, specifically isoform Br-Z4, is involved in
294 the regulation of the expression of *drs* at pupariation.
295

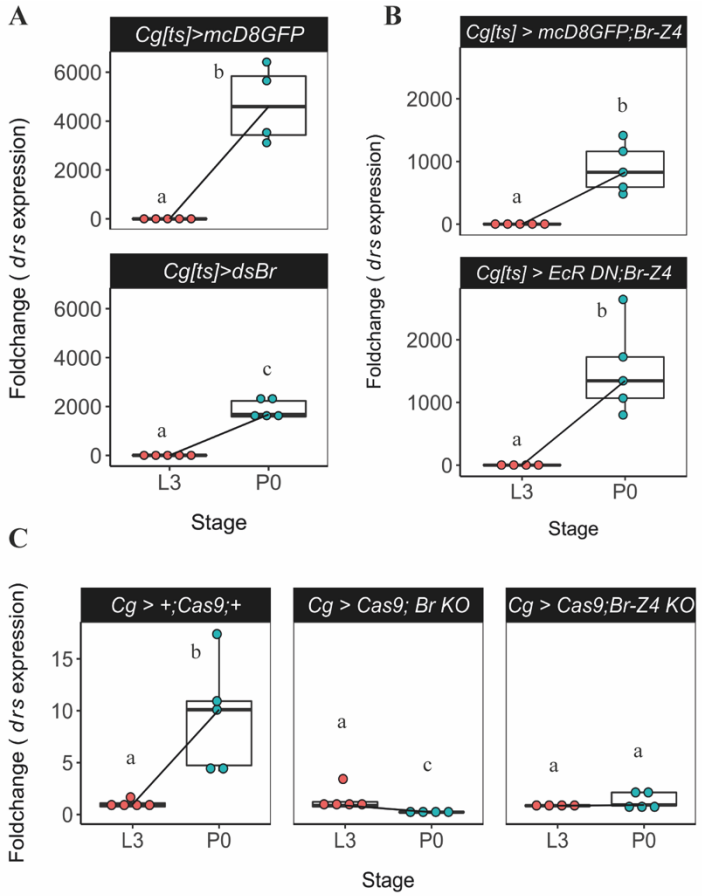

296
297 **Fig 3. Ecdysone signalling regulates fat body expression of *drs* at pupariation via Br-Z4. (A)**
298 Knockdown of *br* specifically in the fat body and haemocytes leads to decreased expression of *drs* at
299 P0. (**B**) Co-overexpression of *br-Z4* when ecdysone sensitivity is decreased in the fat body and
300 haemocytes is sufficient to rescue the expression of *drs* at pupariation (**C**) Conditional CRISRP-
301 mediated knock-outs for the common region of *br* and *br-Z4* lead to loss of *drs* expression at
302 pupariation. Each dot represents a sample of five pooled individuals; the lines connect the median of

303 the samples at L3 and P0; different letters represent statistically significant differences in foldchange,
304 determined using the ΔΔCT method.

305 Discussion

306 In this study we explored the association between ecdysone and the increased expression
307 of *drs* and its paralogues at pupariation and the biological consequence of this process. We
308 unravelled a *in vivo* association, to our knowledge yet undescribed, between the endocrine and
309 immune systems in *D. melanogaster*, which act both systemically and locally during
310 metamorphosis, emphasizing the biological relevance of the association between ecdysone
311 signalling and AMP expression. Importantly, we could determine that the systemic expression of
312 *drs* has an effect on the number of bacteria during metamorphosis, as both mutant and ecdysone-
313 reduced sensitivity individuals showed an increase rather than a decrease in the number of bacteria
314 between P0 and pharate adult stages. Interestingly the effect was detected for both Gram-positive
315 (*Lactobacillus*) and Gram-negative (*Acetobacter*) bacteria. Although Drs is generally
316 characterized as an antifungal AMP, previous studies already demonstrated that it can also be
317 induced by both Gram-positive and Gram-negative bacteria [36–42]. As such, the unexpected
318 higher impact of the lack of *drs* on *Acetobacter* could actually be explained by its possible direct
319 impact on Gram-negative bacteria. Of note that the humoral arm of defence is not the only one
320 acting at this stage of development. Regan and colleagues demonstrated that at pupariation,
321 ecdysone is required to activate haemocytes and to orchestrate the active migration of these cells
322 towards wounding sites [6]. Therefore, at this stage both ecdysone-regulated cellular and humoral
323 mechanisms act in synergy to decrease the probability of infection.
324 Because the lack of local expression of *drsl2* did not affect bacterial persistence *per se* in
325 our conditions, we focused our efforts on trying to disentangle the molecular regulation of *drs*
326 expression in the fat body. We showed that the expression of *drs* at this stage depends upon the
327 expression in the fat body of the ecdysone receptor target, *br-Z4*. This is in accordance to previous
328 indications that Br is essential for the PGRP-LC-independent hormonal regulation of *drs* in S2

329 cells [4]. However, these previous studies did not demonstrate this association *in vivo* and did not
330 explore the temporal importance between the regulation of AMPs by Br and the pupae
331 susceptibility. Furthermore, similar ecdysone-mediated immune activation through Br has been
332 previously observed. Studies in the silkworm *B. mori* showed that during metamorphosis,
333 ecdysone activates the transcription of lysozyme via Br-Z2 [43] and of the AMP *lebocin* via Br-Z4
334 [32]. This regulatory mechanism through Br may cause the stage specificity. Although ecdysone
335 controls all the moults throughout development, *drs* expression increases in response to this
336 hormone specifically at pupariation, when Br is expressed in Holometabola [25,44]. The
337 regulation of AMPs by Br is an interesting feature, as it can also have implications on the
338 interpretation of AMP expression throughout development between holo- and hemimetabolan
339 insects. Johnston [45] demonstrated that these two insect groups have different AMP expression
340 patterns, with holometabolans showing a strong upregulation of immunity that coincides with
341 metamorphosis timing and Br expression. In contrast, hemimetabolans do not undergo a dramatic
342 increase in immunity, possibly correlating with much less drastic changes in gut morphology
343 during progressive metamorphosis. In accordance, there is indication that insects with complete
344 metamorphosis suffer a reduction in density, diversity and altered composition of bacterial
345 populations during metamorphosis [46–48], whereas those with incomplete metamorphosis show
346 a constant increase in microbial density and diversity throughout development [49]. These data, as
347 ours, are consistent with the previously proposed hypothesis that complete metamorphosis elicits a
348 prophylactic immune response [15,16]. However, until now it was unclear how ecdysone could
349 temporally regulate the expression of AMPs at pupariation.
350 Alterations in immunity at life stages with higher risk of infection seem to be a general
351 feature of development, finding some parallels in both vertebrates and invertebrates. In *D.*
352 *triauraria*, genes of the *drs* family are induced during diapause, which is also considered to be a
353 more susceptible period [50]. Most interestingly, data from *Xenopus* also point towards an
354 association between the timing of metamorphosis and a shift in the immune response [51]. For
355 example, Major Histocompatibility Complex I (MHC class I) molecules, which bind to peptide

356 fragments derived from pathogens, are first detected at the beginning of metamorphosis [52] and
357 the expression of MHC class II molecules is not triggered if metamorphosis is chemically blocked
358 [53].

359 Together, our data suggests a regulatory mechanism through which ecdysone co-opted the
360 immune system possibly to enhance the success of metamorphic processes. This study reveals a
361 novel association between the endocrine and immune systems in *D. melanogaster*, which act both
362 systemically and locally during metamorphosis. This recruitment of immunity mechanisms by the
363 holometabolan metamorphosis programme presents other interesting features. Three AMPs
364 explain around 95% of the peak observed at the L3 to pupal transition. Interestingly, these three
365 AMPs have been co-opted differently and complementarily to produce, what we interpret as a full-
366 fledged immune prophylactic response. One of them, *drsl2*, was recruited to one of the main
367 exposed surface epithelia of larvae, the midgut, that undergoes extensive remodelling at
368 metamorphosis. Another of the AMPs with increased expression, *drs*, is produced in the fat body
369 at metamorphosis initiation, executing a putatively systemic action. The local and systemic
370 mechanisms that share ecdysone control and that were explored in this work account for the
371 expression of the genes that constitute close to 70% of the pupariation AMP peak.

372 This specificity and multi-layered developmentally-regulated immune response
373 underscores the sophistication of the co-option process and hints at a possible contribution of this
374 response to the success of metamorphosis as a whole.

375 Materials and methods

376 *Drosophila* stocks and husbandry

377 If not further noticed, *w[1118]* flies were obtained from Dr. Luís Teixeira (Instituto Gulbenkian de
378 Ciência, Portugal) and used as a wild-type strain. The following lines were obtained from the
379 Bloomington Drosophila Stock Center: *w;UAS-mCD8GFP* (#5137), *Cg-Gal4* (#7011), *tub-*

380 *Gal80[ts]*(#7017), *w; UAS-Cas9 P2*(#58986), *w;UAS-brZ4* (#51193) and *w;UAS-dsBroad*
381 (#104648). Several stocks were generously shared by our colleagues, Drs Lynn Riddiford,
382 University of Washington, USA (*w;UAS-EcRADN TP3 W650A*), Marc Dionne, Imperial College
383 London, UK (*Hml-Gal4*), François Leulier, IGFL, France (*Mex-Gal4*), Kim Rewitz, Univeristy of
384 Copenhagen, Denmark (*AkhR-Gal4*), Bruno Lemaitre, EPFL, Switzerland (*iso;iso;Drs*$^{r(w+)}$ and the
385 respective background control). The rescue lines *w;UAS-mCD8GFP; P{UAS-br.Z4}37-6* and
386 *w;UAS-EcRADN TP3 W650A; P{UAS-br.Z4}37-6* were generated in house by the Fly
387 Transgenesis Service (Dr Gastón Guilgur). Standardly raised flies were kept on food with the
388 following composition (g/mL): 4,5% molasse, 7,5% sugar, 7% cornmeal, 2% yeast extract, 1%
389 agar, 2,5% Nipagin 10%. All fly lines we kept at 25ºC in a 12L:12D photoperiod. For the
390 ecdysone decreased sensitivity experiment and tissue specific CRISPR, animals were maintained
391 at 17ºC until the moult to the L3 and then transferred to 29ºC to activate Gal4 activity.

392 CRISPR knock-out flies generation

393 The tissue-specific UAS *br* CRISPR knockout constructs were cloned into pCFD6 vector
394 (www.crisprflydesign.org, Addgene #73915) according to manufacturer's instructions. Four
395 independent gRNA constructs were cloned to target introns (see primers listed in S7 Table) of the
396 *br* core region genomic DNA sequence for *br* common construct and Z4 isoform specific
397 sequence for *br-Z4* construct to target only native genes but not transgenes. After sequenced, the
398 constructs were inserted on either the second chromosome in a recipient line carrying phiC31
399 integrase and attP40 landing cite with an in-house modified line (*y,w, P{y+.nos-int.NLS};*
400 *P{CaryP y+}attP40*) or the third chromosome in a recipient line carrying phiC31 integrase and
401 attP2 landing site, *y,w, P(y[+].nos-int. NLS); P(CaryP)attP2* (gift from Dr. Diogo Manoel, Sidra
402 Medical and Research Center, Qatar). Transgenesis was carried out in-house at the Instituto
403 Gulbenkian de Ciência, Portugal.

404 # Larval and pupal staging

405 Larvae were resynchronized every 2h and kept in normal food for the appropriate time before
406 collection in Trizol. White pre-pupae (P0) were identified as motionless pre-pupae with
407 evaginated anterior spiracles and collected directly in Trizol every 20 minutes. All samples were
408 kept at -80ºC until use. Egg collections were performed on standard *Drosophila* food plates at
409 25ºC, unless mentioned otherwise. All larvae used for this study were resynchronised either at the
410 onset of the L2 or L3, as previously described [54]. Eggs were collected every 4 hours and larval
411 densities kept around 200 larvae/60 mm diameter plate. Newly moulted L2 or L3 larvae were
412 collected every 2 hours. Collected larvae (up to a maximum of 30 larvae/vial) were raised in vials
413 with standard food at 25°C for an additional twenty-four hours. Staged larvae were collected in
414 Trizol for RNA extraction and stored at -80ºC until use. For collection of P0, bottles with L3
415 larvae were monitored every 20 minutes, between 48 and 72h after the moult to the L3. Across
416 this study, white pre-pupae (P0) were identified as motionless pre-pupae with evaginated anterior
417 spiracles. After collection, samples were immediately stored in Trizol and stored at -80ºC until
418 RNA extraction.

419 # P0 and pharate adult collection and platting

420 P0 samples were collected as aforementioned. Pharate adults were identified as fully developed
421 adults (with tanned wings and pigmented eyes) still to eclose. Pharate adults were dissected out of
422 the pupal case and collected in 20 minutes intervals 48h to 72h after P0 collection. All samples
423 were surface sterilized once with Milli-Q water, 70% ethanol and 13% bleach and rinsed (3x) with
424 sterile water to eliminate bleach traces. After these treatments, each pupa was macerated in 300
425 µL of LB medium, of which 50 µL were spread onto MRS or D-Mannitol plates. The plates were
426 incubated at 25ºC for 48h for bacterial growth. For each stage and medium a sample size of 100
427 pupae/pharate was collected per genotype.

428 # Statistical analysis for bacterial growth across stages

429 To compare the pattern of variation between P0 and pharate adults across genotypes, we followed
430 a resampling strategy [55]: the initial sample was resampled in subsets of 50 entries, with no
431 replacement, 2000 times, generating a simulated dataset. In each cycle, a negative binomial
432 regression (*glm.nb(datat$cfu_pupae ~ data$Stage)*) – which does not assume that the variance and
433 the mean of the data to be equivalent - was performed to model the change of bacteria according
434 to the stage, generating a regression coefficient, or slope.
435 At the end of the 2000th cycle, a set of these coefficients was obtained for each genotype. This
436 strategy allows us to estimate a set of values that the negative binomial generalized linear
437 regressions may assume, instead of getting just one value. In turn, this set can allow us to explore
438 location and variation statistics, as well as better estimate the parameters of the sampling
439 distribution of the coefficients, with a better notion of its precision.
440 Subsequently, we assessed if the central tendency of the population is greater or less than 0 using
441 one-sided hypothesis tests. In parallel, a measure of the effect size was also calculated. Following
442 a Shapiro-Wilk test of normality, a parametric or non-parametric approach for hypothesis testing
443 and effect size calculation was applied. All data was analysed and all graphics were generated
444 using Rstudio 1.2.5033.

445 # Germ-free fly generation

446 Newly laid eggs were collected into a sterile embryo basket and washed with autoclaved MilliQ
447 water. The eggs were dechorionated and sterilised using a 13% Bleach solution (Sigma Aldrich®)
448 for 10 minutes, washed again with Milli-Q water and sterilized using a 1% Virkon solution for 2
449 minutes. The sterilized embryos were transferred to axenic media with or without antibiotics (200
450 mg/mL Rifampicin, 100 mg/mL Tetracycline, 100 mg/mL Streptomycin, 15 mg/mL gentamicin).
451 The axenic media contained all the normal ingredients of fly food, being autoclaved prior to use
452 and supplemented with the fungicide Bavistin. All plates and bottles were kept inside sterilised

453 containers at 25ºC and all manipulations were conducted in a horizontal flood hood, using sterile
454 materials.
455 After the treatment, the germ-free status was validated by plating surface-sterilized adult flies
456 (from both germ free and control conditions) onto MRS and D- Mannitol media.

457 RNA extraction, cDNA synthesis and real-quantitative PCR

458 RNA was isolated using the Direct-zol™ RNA MiniPrep Kit (Zymo®), following manufacturer's
459 instructions. DNase I treatment and cDNA synthesis were preformed using the RQ1 RNASE-
460 FREE DNASE 1* (Promega®) and the RevertAid H Minus First Strand cDNA Synthesis Kit
461 (Thermo Scientific®), respectively. qPCR was performed using the SYBR® Green PCR Master
462 Mix (Applied Biosystems®) and ABI 7900HT (Applied Biosystems). The PCR conditions used in
463 all experiments were: initial denaturation/ enzyme activation, 95ºC for 10'; followed by 45 cycles
464 of denaturation, 95ºC for 10"; annealing, 60ºC for 10"; extension, 72ºC for 30". Specificity of
465 PCR amplification was verified by melting curve: 95ºC for 10", 65ºC for 1', 97ºC for 1"; cooling,
466 37ºC, 30". Primers used for all qPCR reactions are represented in S10 Table. Foldchange was
467 determined using the ΔΔCT method, which compares the expression of a given gene of interest to
468 a housekeeping gene between experimental and control samples [56,57]. Control L3 samples
469 were used as reference. The data was analysed with a general linear model, using the genotype,
470 stage and gene as explicable variables, as follows: glm(log(Foldchange)~Genotype*Stage*Gene,
471 data=mydata). The expression level for each gene at P0 and pharate was compared within and
472 between genotypes through multiple comparisons using the *lsmeans* package from Rstudio
473 1.2.5033.

474 Br binding sites prediction

475 The DNA binding motif matrix for Br-Z4 was obtained from the JASPAR database
476 (http://jaspar.genereg.net) and the 5' 2kb region of the *drosomycin* gene was acquired in Flybase

(http://flybase.org). Both sequences were uploaded in FIMO software (http://meme-suite.org/tools/fimo) [33], using a p-value < 0.0001 as a filter.

Acknowledgments

We thank Drs. Lynn Riddiford, Marc Dionne, Luís Teixeira, Bruno Lemaitre, François Leulier, Kim Rewitz and Pedro Domingos for stock sharing. We thank Liliana Vieira and Sandra Crisóstomo for technical assistance, Gastón Guilgur for transgenesis services and André Barros for help with statistical analysis. Stocks obtained from the Bloomington Drosophila Stock Center (NIH P40OD018537) were used in this study. This work was supported by: Instituto Gulbenkian de Ciência/Fundação Calouste Gulbenkian; Fundação para a Ciência e a Tecnologia (FCT, Portugal) to CN (PD/BD/114344/2016); CONGENTO, project LISBOA-01-0145-FEDER-022170, co-financed by Lisboa Regional Operational Programme (Lisboa 2020), under the Portugal 2020 Partnership Agreement, through the European Regional Development Fund (ERDF), and Fundação para a Ciência e a Tecnologia (FCT, Portugal).

References

1. Nijhout HF. Insect hormones. Princept: Princeton University Press; 1994.
2. Gilbert, L. I., Rybczynski, R., Tobe SS. Endocrine cascade in insect metamorphosis. In: Gilbert, L.I., Tata, J.R., Atkinson BG, editor. Metamorphosis, postembryonic reprogramming of gene expression in amphibian and insect cells. Academic Press Inc; 1996. pp. 59–107. doi:10.1016/b978-012283245-1/50004-x
3. Webster JI, Tonelli L, Sternberg EM. Neuroendocrine regulation of immunity. Annu Rev Immunol. 2002;20: 125–163. doi:10.1146/annurev.immunol.20.082401.104914
4. Rus F, Flatt T, Tong M, Aggarwal K, Okuda K, Kleino A, et al. Ecdysone triggered PGRP-LC expression controls Drosophila innate immunity. EMBO J. Nature Publishing Group; 2013;32: 1626–1638. doi:10.1038/emboj.2013.100

501 5. Flatt T, Heyland A, Rus F, Porpiglia E, Sherlock C, Yamamoto R, et al. Hormonal regulation
502 of the humoral innate immune response in Drosophila melanogaster. J Exp Biol. 2008;211:
503 2712–2724. doi:10.1242/jeb.014878
504 6. Regan JC, Brandão AS, Leitão AB, Mantas Dias ÂR, Sucena É, Jacinto A, et al. Steroid
505 hormone signaling is essential to regulate innate immune cells and fight bacterial infection in
506 Drosophila. PLoS Pathog. 2013;9. doi:10.1371/journal.ppat.1003720
507 7. Dimarcq JL, Imler JL, Lanot R, Ezekowitz RAB, Hoffmann JA, Janeway CA, et al. Treatment
508 of l(2)mbn Drosophila tumorous blood cells with the steroid hormone ecdysone amplifies the
509 inducibility of antimicrobial peptide gene expression. Insect Biochem Mol Biol. 1997;27: 877–
510 886. doi:10.1016/S0965-1748(97)00072-6
511 8. Wang JL, Chen L, Tang L, Zhao HB, Liu XS, Wang YF. 20-hydroxyecdysone transcriptionally
512 regulates humoral immunity in the fat body of Helicoverpa armigera. Insect Mol Biol. 2014;23:
513 842–856. doi:10.1111/imb.12131
514 9. Nunes C, Sucena É, Koyama T. Endocrine regulation of immunity in insects. FEBS J. 2020; 1–
515 20. doi:10.1111/febs.15581
516 10. Hoffmann JA, Reichhart JM, Hetru C. Innate immunity in higher insects. Curr Opin Immunol.
517 1996;8: 8–13. doi:10.1016/S0952-7915(96)80098-7
518 11. Du Pasquier L. The immune system of invertebrates and vertebrates. Comp Biochem Physiol -
519 B Biochem Mol Biol. 2001;129: 1–15. doi:10.1016/S1096-4959(01)00306-2
520 12. Lemaitre B, Hoffmann J. The host defense of Drosophila melanogaster. Annu Rev Immunol.
521 2007;25: 697–743. doi:10.1146/annurev.immunol.25.022106.141615
522 13. Cociancich S, Bulet P, Hetru C, Hoffmann JA. The inducible antibacterial peptides of insects.
523 Parasitol Today. 1994;10: 132–139. doi:10.1016/0169-4758(94)90260-7
524 14. Yu XQ, Kanost MR. Developmental expression of Manduca sexta hemolin. Arch Insect
525 Biochem Physiol. 1999;42: 198–212. doi:10.1002/(SICI)1520-6327(199911)42:3<198::AID-
526 ARCH4>3.0.CO;2-G
527 15. Russell VW, Dunn PE. Lysozyme in the midgut of Manduca sexta during metamorphosis.
528 1991;80: 67–80.
529 16. Russell V, Dunn PE. Antibacterial proteins in the midgut of Manduca sexta during

530 metamorphosis. J Insect Physiol. 1996;42: 65–71. doi:10.1016/0022-1910(95)00083-6
531 17. Hakim RS, Baldwin K, Smagghe G. Regulation of midgut growth, development, and
532 metamorphosis. Annu Rev Entomol. 2010;55: 593–608. doi:10.1146/annurev-ento-112408-
533 085450
534 18. Judy KJ, Gilbert LI. Histology of the alimentary canal during the metamorphosis of
535 Hyalophora cecropia (L.). J Morphol. 1970;131: 277–299. doi:10.1002/jmor.1051310304
536 19. Bacot A. On the persistence of Bacilli in the gut of an Insect during metamorphosis.
537 Parasitology. 1911;4: 497–500.
538 20. Leach JG. The method of survival of bacteria in the puparia of the seed-corn maggot
539 (Hylemyia Cilicrura Rond.). Zeitschrift für Angew Entomol. 1934;20: 150–161.
540 doi:10.1111/j.1439-0418.1934.tb00358.x
541 21. Bakula M. The persistence of a microbial flora during postembryogenesis of Drosophila
542 melanogaster. J Invertebr Pathol. 1969;14: 365–374. doi:10.1016/0022-2011(69)90163-3
543 22. Duneau DF, Lazzaro BP. Persistence of an extracellular systemic infection across
544 metamorphosis in a holometabolous insect. Biol Lett. 2018;14: 10–13.
545 doi:10.1098/rsbl.2017.0771
546 23. Thurmond J, Goodman JL, Strelets VB, Attrill H, Gramates LS, Marygold SJ, et al. FlyBase
547 2.0: The next generation. Nucleic Acids Res. Oxford University Press; 2019;47: D759–D765.
548 doi:10.1093/nar/gky1003
549 24. Zhang Z, Palli SR. Identification of a cis-regulatory element required for 20-hydroxyecdysone
550 enhancement of antimicrobial peptide gene expression in Drosophila melanogaster. Insect Mol
551 Biol. 2009;18: 595–605. doi:10.1111/j.1365-2583.2009.00901.x
552 25. Zhou X, Riddiford LM. Broad specifies pupal development and mediates the “status quo”
553 action of juvenile hormone on the pupal-adult transformation in Drosophila and Manduca.
554 Development. 2002;129: 2259–2269.
555 26. Cherbas L, Hu X, Zhimulev I, Belyaeva E, Cherbas P. EcR isoforms in Drosophila: Testing
556 tissue-specific requirements by targeted blockade and rescue. Development. 2003;130: 271–
557 284. doi:10.1242/dev.00205
558 27. Buchon N, Broderick NA, Poidevin M, Pradervand S, Lemaitre B. Drosophila Intestinal

559 Response to Bacterial Infection: Activation of Host Defense and Stem Cell Proliferation. Cell
560 Host Microbe. Elsevier Ltd; 2009;5: 200–211. doi:10.1016/j.chom.2009.01.003
561 28. Truman JW, Riddiford LM. The origins of insect metamorphosis. Nature. 1999;401: 447–452.
562 Available: http://dx.doi.org/10.1038/46737
563 29. Belles X. Origin and evolution of insect metamorphosis. eLS. 2011; 1–11.
564 doi:10.1002/9780470015902.a0022854
565 30. Port F, Chen HM, Lee T, Bullock SL. Optimized CRISPR/Cas tools for efficient germline and
566 somatic genome engineering in Drosophila. Proc Natl Acad Sci U S A. 2014;111.
567 doi:10.1073/pnas.1405500111
568 31. Xue Z, Wu M, Wen K, Ren M, Long L, Zhang X, et al. CRISPR/Cas9 mediates efficient
569 conditional mutagenesis in Drosophila. G3 Genes, Genomes, Genet. 2014;4: 2167–2173.
570 doi:10.1534/g3.114.014159
571 32. Mai T, Chen S, Lin X, Zhang X, Zou X, Feng Q, et al. 20-hydroxyecdysone positively
572 regulates the transcription of the antimicrobial peptide, lebocin, via BmEts and BmBR-C Z4 in
573 the midgut of Bombyx mori during metamorphosis. Dev Comp Immunol. Elsevier Ltd;
574 2017;74: 10–18. doi:10.1016/j.dci.2017.04.002
575 33. Grant CE, Bailey TL, Noble WS. FIMO: Scanning for occurrences of a given motif.
576 Bioinformatics. 2011;27: 1017–1018. doi:10.1093/bioinformatics/btr064
577 34. Dunn PE. Humoral immunity in insects. Bioscience. 1990;40: 738–744. doi:10.2307/1311506
578 35. Hultmark D. Immune reactions in Drosophila and other insects: a model for innate immunity.
579 Trends Genet. 1993;9: 178–183. doi:10.1016/0168-9525(93)90165-E
580 36. Tzou P, Ohresser S, Ferrandon D, Capovilla M, Reichhart J, Lemaitre B, et al. Tissue-specific
581 inducible expression of antimicrobial peptide genes in Drosophila surface epithelia. 2000;13:
582 737–748.
583 37. Lemaitre B, Reichhart JM, Hoffmann JA. Drosophila host defense: Differential induction of
584 antimicrobial peptide genes after infection by various classes of microorganisms. Proc Natl
585 Acad Sci U S A. 1997;94: 14614–14619. doi:10.1073/pnas.94.26.14614
586 38. Leulier F, Rodriguez A, Khush RS, Abrams JM, Lemaitre B. The Drosophila caspase Dredd is
587 required to resist Gram-negative bacterial infection. EMBO Rep. 2000;1: 353–358.

588 doi:10.1093/embo-reports/kvd073
589 39. Foley E, O'Farrell PH. Nitric oxide contributes to induction of innate immune responses to
590 gram-negative bacteria in Drosophila. Genes Dev. 2003;17: 115–125.
591 doi:10.1101/gad.1018503
592 40. Tanji T, Hu X, Weber ANR, Ip YT. Toll and IMD pathways synergistically activate an innate
593 Immune Response in Drosophila melanogaster. Mol Cell Biol. 2007;27: 4578–4588.
594 doi:10.1128/mcb.01814-06
595 41. Li Y, Li S, Li R, Xu J, Jin P, Chen L, et al. Genome-wide miRNA screening reveals miR-310
596 family members negatively regulate the immune response in Drosophila melanogaster via co-
597 targeting Drosomycin. Dev Comp Immunol. Elsevier Ltd; 2017;68: 34–45.
598 doi:10.1016/j.dci.2016.11.014
599 42. Zhan MY, Yang PJ, Rao XJ. Molecular cloning and analysis of PGRP-L1 and IMD from
600 silkworm Bombyx mori [Internet]. Comparative Biochemistry and Physiology Part - B:
601 Biochemistry and Molecular Biology. Elsevier Inc; 2018. doi:10.1016/j.cbpb.2017.10.002
602 43. Ma H, Abbas MN, Zhang K, Hu X, Xu M, Liang H, et al. 20-Hydroxyecdysone regulates the
603 transcription of the lysozyme via Broad-Complex Z2 gene in silkworm, Bombyx mori. Dev
604 Comp Immunol. Elsevier; 2019;94: 66–72. doi:10.1016/j.dci.2019.01.014
605 44. Erezyilmaz DF, Riddiford LM, Truman JW. The pupal specifier broad directs progressive
606 morphogenesis in a direct-developing insect. Proc Natl Acad Sci U S A. 2006;103: 6925–6930.
607 doi:10.1073/pnas.0509983103
608 45. Johnston PR, Paris V ronique, Rolff J. Immune gene regulation in the gut during
609 metamorphosis in a holo- versus a hemimetabolous insect. Philos Trans R Soc B Biol Sci.
610 2019;374: 1–6. doi:10.1098/rstb.2019.0073
611 46. Johnston PR, Rolff J. Host and Symbiont Jointly Control Gut Microbiota during Complete
612 Metamorphosis. PLoS Pathog. 2015;11: 1–11. doi:10.1371/journal.ppat.1005246
613 47. Hammer TJ, McMillan WO, Fierer N. Metamorphosis of a butterfly-associated bacterial
614 community. PLoS One. 2014;9. doi:10.1371/journal.pone.0086995
615 48. Kim JK, Han SH, Kim CH, Jo YH, Futahashi R, Kikuchi Y, et al. Molting-associated
616 suppression of symbiont population and up-regulation of antimicrobial activity in the midgut

symbiotic organ of the Riptortus-Burkholderia symbiosis. Dev Comp Immunol. Elsevier Ltd; 2014;43: 10–14. doi:10.1016/j.dci.2013.10.010

49. Sudakaran S, Salem H, Kost C, Kaltenpoth M. Geographical and ecological stability of the symbiotic mid-gut microbiota in European firebugs, Pyrrhocoris apterus (Hemiptera, Pyrrhocoridae). Mol Ecol. 2012;21: 6134–6151. doi:10.1111/mec.12027

50. Daibo S, Kimura MT, Goto SG. Upregulation of genes belonging to the drosomycin family in diapausing adults of Drosophila triauraria. Gene. 2001;278: 177–184. doi:10.1016/S0378-1119(01)00713-2

51. Robert J, Ohta Y. Comparative and developmental study of the immune system in Xenopus. Dev Dyn. 2009;238: 1249–1270. doi:10.1002/dvdy.21891

52. Flajnik MF, Du Pasquier L. MHC class I antigens as surface markers of adult erythrocytes during the metamorphosis of Xenopus. Dev Biol. 1988;128: 198–206. doi:10.1016/0012-1606(88)90282-5

53. Rollins-Smith LA, Blair P. Expression of class II major histocompatibility complex antigens on adult T cells in Xenopus is metamorphosis-dependent. Dev Immunol. 1990;1: 97–104.

54. Koyama T, Mirth CK. Growth-Blocking Peptides As Nutrition-Sensitive Signals for Insulin Secretion and Body Size Regulation. PLoS Biol. 2016;14: 1–23. doi:10.1371/journal.pbio.1002392

55. Fieberg JR, Vitense K, Johnson DH. Resampling-based methods for biologists. PeerJ. 2020;2020. doi:10.7717/peerj.9089

56. Livak KJ, Schmittgen TD. Analysis of relative gene expression data using real-time quantitative PCR and the 2-ΔΔCT method. Methods. 2001;25: 402–408. doi:10.1006/meth.2001.1262

57. Schmittgen TD, Livak KJ. Analyzing real-time PCR data by the comparative CT method. Nat Protoc. 2008;3: 1101–1108. doi:10.1038/nprot.2008.73

Supporting Information

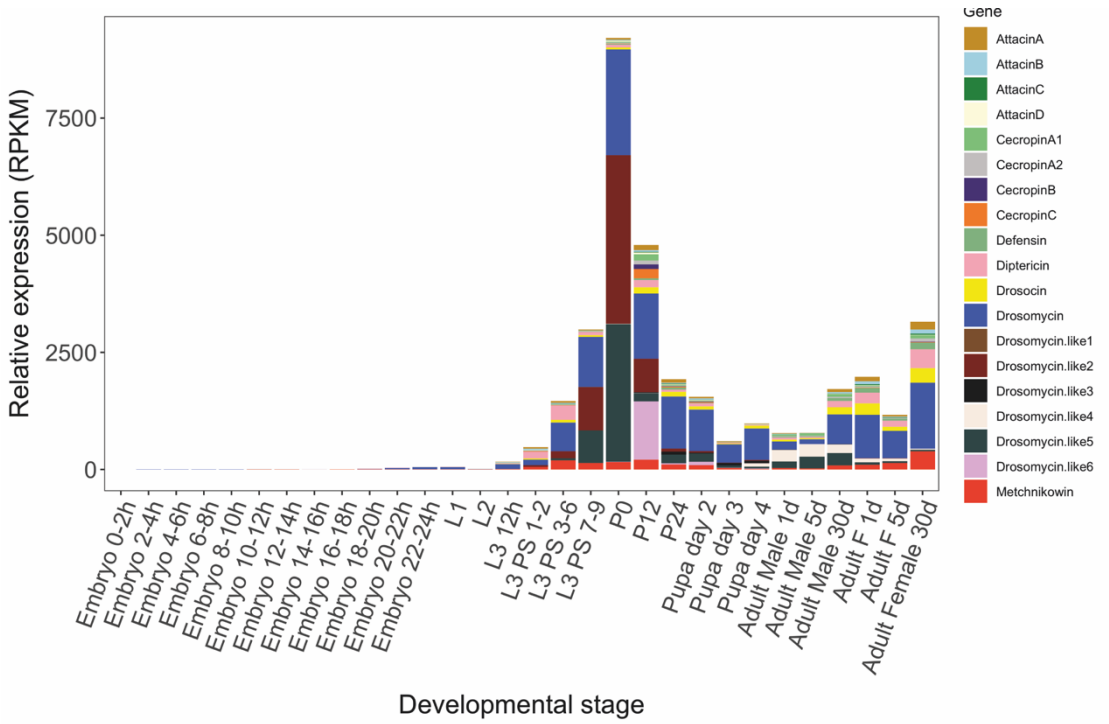

S1 Fig. High-throughput temporal AMP expression. Expression refers to whole body, with levels represented as linear and scaled to maximum expression (publicly available on Flybase http://flybase.org/ [23]).

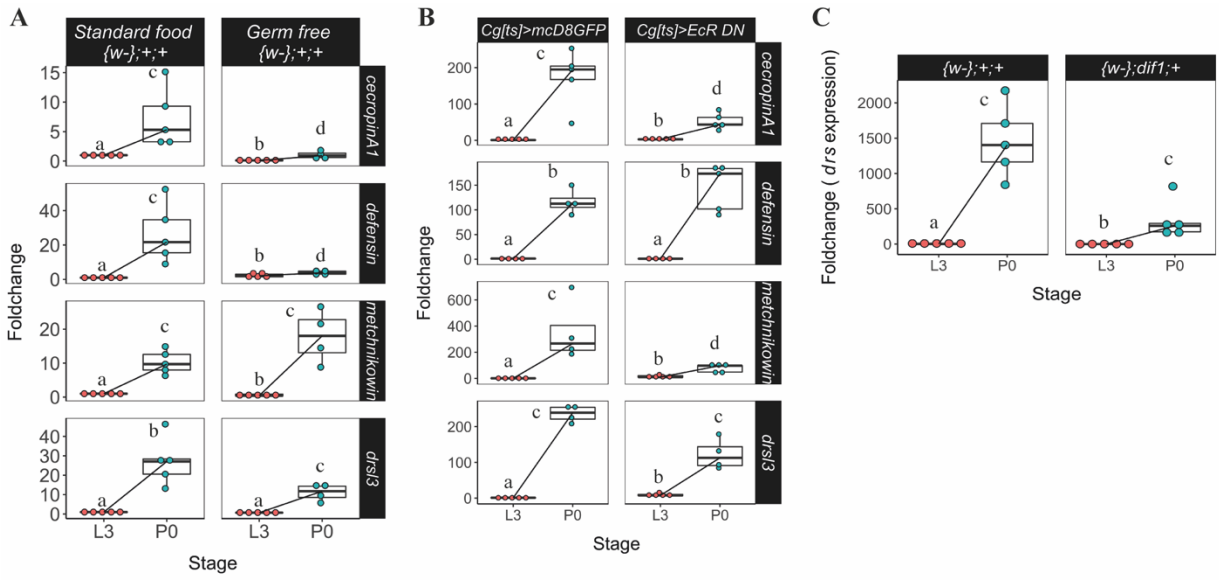

650 **S2 Fig. Expression of other four AMPs is not loss under GF or ecdysone reduced sensitivity**
651 **conditions. (A)** The expression levels of *cecropin A1, defensin, metchnikowin* and *drsl3* increase at
652 pupariation and are not lost in GF conditions, albeit to different degrees. **(B)** Reduced expression of
653 ecdysone sensitivity in the fat body and haemocytes does not affect the expression of *cecropin A1,*
654 *defensin, metchnikowin* and *drsl3*. (**C**) *drs* expression still increases at P0 in dif1 mutant flies. Each dot
655 represents a sample of five pooled individuals; the lines connect the median of the samples at L3 and
656 P0; different letters represent statistically significant differences in foldchange. Foldchange was
657 determined using the ΔΔCT method.
658

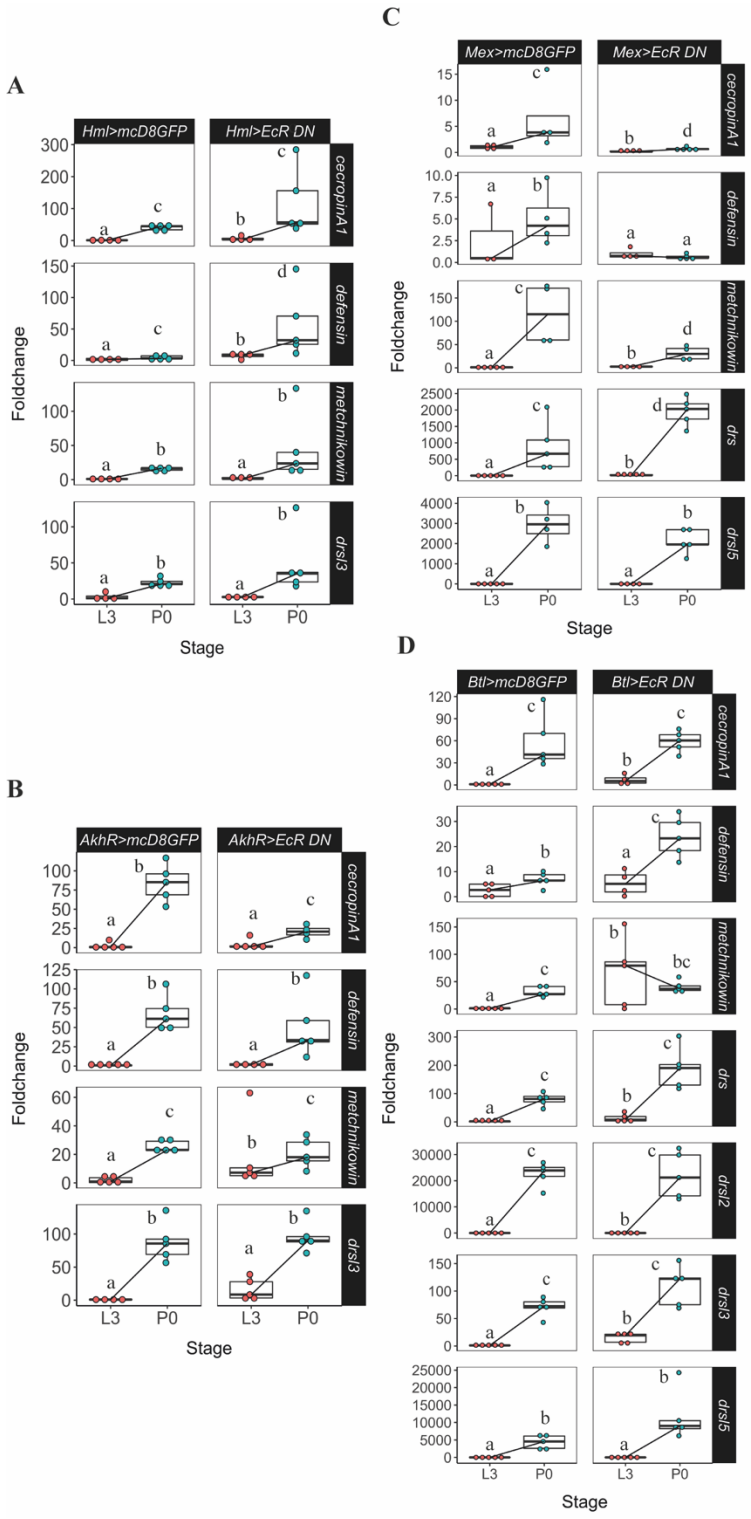

659

660 **S3 Fig. Reduced ecdysone sensitivity in haemocytes, fat body, midgut and trachea does not alter**

661 **AMP expression. (A)** Reduced ecdysone sensitivity in the haemocytes does not affect the expression

662 of the AMPs under study. **(B)** The expression of *cecropin A1, defensin, metchnikowin* and *drsl3* was

663 unaffected by decreased ecdysone sensitivity specifically in the fat body. **(C)** Decreased ecdysone

signalling in the midgut resulted in significant decrease in mRNA levels for: *cecropin A1* (*lsmeans(pairwise~Genotype|P0)<0.0001; lsmeans(pairwise~Stage|Mex>EcRDN)= 0.0038), defensin (lsmeans(pairwise~Genotype|P0) <0.0001; lsmeans(pairwise~Stage|Mex>EcR DN)=0.3866), metchnikowin* (*lsmeans (pairwise~Genotype|P0)=0.0060; lsmeans (pairwise~Stage|Mex>EcRDN<0.0001*), and *drsl3 ((lsmeans(pairwise~Genotype|P0)=0.0008; lsmeans(pairwise~Stage|Mex>EcRDN)=0.2084*). **(D)** Ecdysone signalling in the trachea does not affect the expression of any AMP under study.

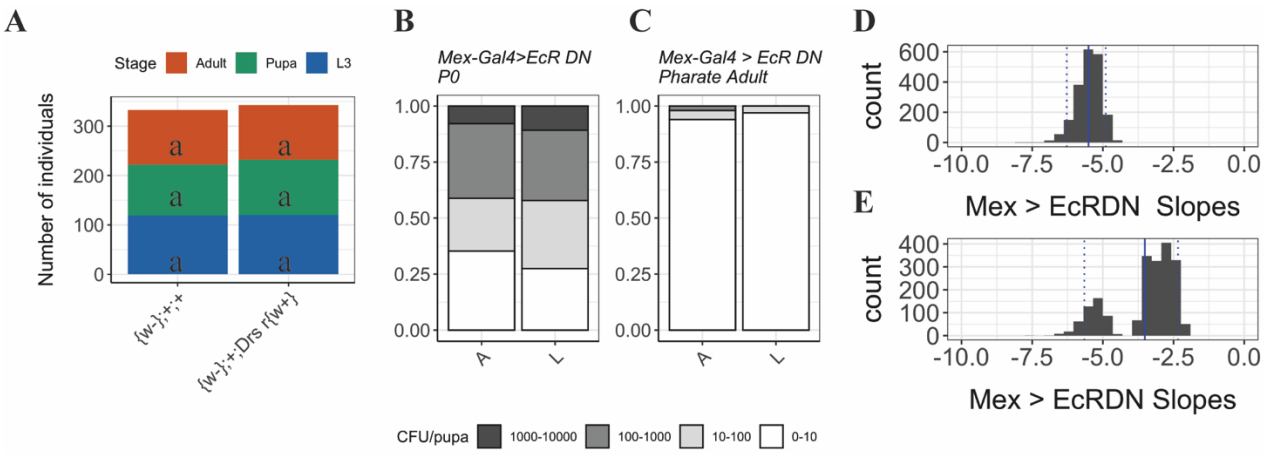

S4 Fig. Local loss of *drsl2* does not affect bacterial clearance during metamorphosis. (A) Control ({*w-*};+;+) and *drs* mutant ({*w-*};+; *Drs r*{*w+*}) lines showed no differences in mortality between L3, pupae and adults (*lsmeans(pairwise~Stage|Genotype)<0.0001; lsmeans(pairwise~Genotype|Stage)<0.0001*). **(B-C)** Quantification in P0 pupae and pharate adults of *Lactobacillus* (L), growing in selective MRS medium, and *Acetobacter* (A), growing on selective D-Mannitol. The number of individuals with more bacteria is greater in P0 samples **(B)** than in pharate adults **(C).** Y-axis represents the proportion of individuals in each bacterial count category. **(D-E)** Coefficient (slopes) distribution in *Mex>EcRDN* samples of *Lactobacillus* **(D)** (*Median: -5.455 (IQR: -6.279; -4.895); One-way Wilcoxon test for median<0: <2.2e-16, r=0.866*) and *Acetobacter* **(E)** (*Median: -3.134 (IQR: -5.656; -2.342); One-way Wilcoxon test for median>0: <2.2e-16, r=0.866).* Doted lines represent the 0.05 and 0.95 quantiles; full line represents the mean slope.

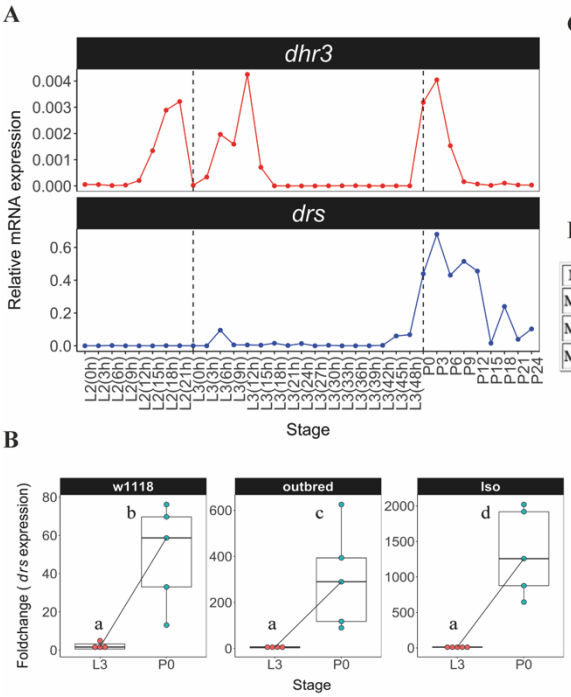

D

Motif ID	Alt ID	Sequence Name	Strand	Start	End	p-value	q-value	Matched Sequence
MA0013.1	br(var.4)	Drs	+	1022	1032	8.65e-06	0.0254	AAGTAAACAAA
MA0013.1	br(var.4)	Drs	-	1189	1199	1.9e-05	0.0279	TAATAAACAAC
MA0013.1	br(var.4)	Drs	+	755	765	7.17e-05	0.0703	TAGAAAAGAAA

S5 Fig. **Br-Z4 is involved in the ecdysone-dependent AMP expression at pupariation.** **(A)** *drs* expression was temporally correlated with a proxy of ecdysone activity, *dhr3*. Samples of *D. melanogaster* larvae and pupae were precisely staged at the onset of the instars and collected every 3h. The expression of *dhr3* and *drs* was determined by qPCR for each timepoint. Dashed black lines represent the moult to the L3 or pupariation. **(B)** The expression of *drs* increased at pupariation regardless of the genetic background (*lsmeans(pairwise~Stage|w1118)<0.0001; lsmeans(pairwise~Stage|outbred<0.0001; lsmeans(pairwise~Stage|Iso)<0.0001*). Each dot represents a sample of five pooled individuals; the lines connect the median of the samples at L3 and P0; different letters represent statistically significant differences in fold-change. Fold-change was determined using the ΔΔCT method. **(C)** JASPAR DNA binding motif MA0013.1 for Br-Z4**. (D)** Br-Z4 binding motifs predicted by FIMO [29] software (http://meme-suite.org/tools/fimo) to be present in 2kb region of the 5'-end of the *drs* gene, using a p-value<0.0001 as filter.

Gene	*lsmeans, pairwise~Genotype | Stage*	*p-value*
cecropin A1	*{w-};+;+* vs *{w-};+;+* GF | L3	<0.0001
	{w-};+;+ vs *{w-};+;+* GF | P0	<0.0001
defensin	*{w-};+;+* vs *{w-};+;+* GF | L3	0.0096
	{w-};+;+ vs *{w-};+;+* GF | P0	<0.0001
metchnikowin	*{w-};+;+* vs *{w-};+;+* GF | L3	0.0089
	{w-};+;+ vs *{w-};+;+* GF | P0	0.1038
drs	*{w-};+;+* vs *{w-};+;+* GF | L3	<0.0001
	{w-};+;+ vs *{w-};+;+* GF | P0	0.0978
drsl2	*{w-};+;+* vs *{w-};+;+* GF | L3	<0.0001
	{w-};+;+ vs *{w-};+;+* GF | P0	0.0226
drsl3	*{w-};+;+* vs *{w-};+;+* GF | L3	0.2113
	{w-};+;+ vs *{w-};+;+* GF | P0	0.0058
drsl5	*{w-};+;+* vs *{w-};+;+* GF | L3	<0.0001
	{w-};+;+ vs *{w-};+;+* GF | P0	0.0105
Gene	***lsmeans, pairwise~Stage | Genotype***	***p-value***
cecropin A1	*{w-};+;+*	<0.0001
	{w-};+;+ GF	<0.0001
defensin	*{w-};+;+*	<0.0001
	{w-};+;+ GF	0.0752
metchnikowin	*{w-};+;+*	<0.0001
	{w-};+;+ GF	<0.0001
drs	*{w-};+;+*	<0.0001
	{w-};+;+ GF	<0.0001
drsl2	*{w-};+;+*	<0.0001
	{w-};+;+ GF	<0.0001
drsl3	*{w-};+;+*	<0.0001
	{w-};+;+ GF	<0.0001
drsl5	*{w-};+;+*	<0.0001
	{w-};+;+ GF	<0.0001

S1 Table. **Statistical analysis of AMPs expression in an isogenic line (*{w-};+;+*) both in normal and germ-free (GF) conditions**. lsmeans, pairwise~Genotype | Stage represents differences within the same stage, between genotypes. lsmeans, pairwise~Stage | Genoype represents the difference between L3 and P0 within each genotype.

Gene	lsmeans, pairwise~Genotype | Stage	p-value
cecropin A1	*Cg[ts]>mcD8GFP* vs *Cg[ts]>EcR DN* | L3	0.0057
	Cg[ts]>mcD8GFP vs *Cg[ts]>EcR DN* | P0	0.0064
defensin	*Cg[ts]>mcD8GFP* vs *Cg[ts]>EcR DN* | L3	0.8361
	Cg[ts]>mcD8GFP vs *Cg[ts]>EcR DN* | P0	0.6428
metchnikowin	*Cg[ts]>mcD8GFP* vs *Cg[ts]>EcR DN* | L3	<0.0001
	Cg[ts]>mcD8GFP vs *Cg[ts]>EcR DN* | P0	0.0012
drs	*Cg[ts]>mcD8GFP* vs *Cg[ts]>EcR DN* | L3	0.7558
	Cg[ts]>mcD8GFP vs *Cg[ts]>EcR DN* | P0	<0.0001
drsl2	*Cg[ts]>mcD8GFP* vs *Cg[ts]>EcR DN* | L3	0.6216
	Cg[ts]>mcD8GFP vs *Cg[ts]>EcR DN* | P0	0.0192
drsl3	*Cg[ts]>mcD8GFP* vs *Cg[ts]>EcR DN* | L3	<0.0001
	Cg[ts]>mcD8GFP vs *Cg[ts]>EcR DN* | P0	0.1326
drsl5	*Cg[ts]>mcD8GFP* vs *Cg[ts]>EcR DN* | L3	<0.0001
	Cg[ts]>mcD8GFP vs *Cg[ts]>EcR DN* | P0	0.4561
Gene	**lsmeans, pairwise~Stage | Genotype**	**p-value**
cecropin A1	*Cg[ts]>mcD8GFP* | L3 vs P0	<0.0001
	Cg[ts]>EcR DN | L3 vs P0	<0.0001
defensin	*Cg[ts]>mcD8GFP* | L3 vs P0	<0.0001
	Cg[ts]>EcR DN | L3 vs P0	<0.0001
metchnikowin	*Cg[ts]>mcD8GFP* | L3 vs P0	<0.0001
	Cg[ts]>EcR DN | L3 vs P0	<0.0001
drs	*Cg[ts]>mcD8GFP* | L3 vs P0	<0.0001
	Cg[ts]>EcR DN | L3 vs P0	0..0017
drsl2	*Cg[ts]>mcD8GFP* | L3 vs P0	<0.0001
	Cg[ts]>EcR DN | L3 vs P0	<0.0001
drsl3	*Cg[ts]>mcD8GFP* | L3 vs P0	<0.0001
	Cg[ts]>EcR DN | L3 vs P0	<0.0001
drsl5	*Cg[ts]>mcD8GFP* | L3 vs P0	<0.0001
	Cg[ts]>EcR DN | L3 vs P0	<0.0001

703

704 **S2 Table. Statistical analysis of AMP expression in samples with decreased ecdysone sensitivity in**
705 **the fat body and haemocytes (*Cg>EcR DN*).** lsmeans, pairwise~Genotype | Stage represents
706 differences within the same stage, between genotypes. lsmeans, pairwise~Stage | Genotype represents
707 the difference between L3 and P0 within each genotype.

708

709

Gene	lsmeans, pairwise~Genotype | Stage	p-value
cecropin A1	*Hml>mcD8GFP* vs *Hml>EcR DN* | L3	0.0047
	Hml>mcD8GFP vs *Hml>EcR DN* | P0	0.1124
defensin	*Hml>mcD8GFP* vs *Hml>EcR DN* | L3	0.0012
	Hml>mcD8GFP vs *Hml>EcR DN* | P0	<0.0001
metchnikowin	*Hml>mcD8GFP* vs *Hml>EcR DN* | L3	0.2988
	Hml>mcD8GFP vs *Hml>EcR DN* | P0	0.1739
drs	*Hml>mcD8GFP* vs *Hml>EcR DN* | L3	0.0033
	Hml>mcD8GFP vs *Hml>EcR DN* | P0	0.0185
drsl2	*Hml>mcD8GFP* vs *Hml>EcR DN* | L3	0.0512
	Hml>mcD8GFP vs *Hml>EcR DN* | P0	0.8840
drsl3	*Hml>mcD8GFP* vs *Hml>EcR DN* | L3	0.0732
	Hml>mcD8GFP vs *Hml>EcR DN* | P0	0.3020
drsl5	*Hml>mcD8GFP* vs *Hml>EcR DN* | L3	0.0065
	Hml>mcD8GFP vs *Hml>EcR DN* | P0	0.1605
Gene	**lsmeans, pairwise~Stage | Genotype**	**p-value**
cecropin A1	*Hml>mcD8GFP* | L3 vs P0	<0.0001
	Hml>EcR DN | L3 vs P0	<0.0001
defensin	*Hml>mcD8GFP* | L3 vs P0	0.0118
	Hml>EcR DN | L3 vs P0	0.0003
metchnikowin	*Hml>mcD8GFP* | L3 vs P0	<0.0001
	Hml>EcR DN | L3 vs P0	<0.0001
drs	*Hml>mcD8GFP* | L3 vs P0	<0.0001
	Hml>EcR DN | L3 vs P0	<0.0001
drsl2	*Hml>mcD8GFP* | L3 vs P0	<0.0001
	Hml>EcR DN | L3 vs P0	<0.0001
drsl3	*Hml>mcD8GFP* | L3 vs P0	<0.0001
	Hml>EcR DN | L3 vs P0	<0.0001
drsl5	*Hml>mcD8GFP* | L3 vs P0	<0.0001
	Hml>EcR DN | L3 vs P0	<0.0001

710

711 **S3 Table. Statistical analysis of AMP expression in samples with decreased ecdysone sensitivity in**
712 **haemocytes (*Hml>EcR DN*).** lsmeans, pairwise~Genotype | Stage represents differences within the
713 same stage, between genotypes. lsmeans, pairwise~Stage | Genotype represents the difference between
714 L3 and P0 within each genotype.

715

716

Gene	lsmeans, pairwise~Genotype | Stage	p-value
cecropin A1	*AkhR>mcD8GFP* vs *AkhR>EcR DN* | L3	0.2413
	AkhR>mcD8GFP vs *AkhR>EcR DN* | P0	0.0228
defensin	*AkhR>mcD8GFP* vs *AkhR>EcR DN* | L3	0.4736
	AkhR>mcD8GFP vs *AkhR>EcR DN* | P0	0.3747
metchnikowin	*AkhR>mcD8GFP* vs *AkhR>EcR DN* | L3	0.0001
	AkhR>mcD8GFP vs *AkhR>EcR DN* | P0	0.5902
drs	*AkhR>mcD8GFP* vs *AkhR>EcR DN* | L3	0.0133
	AkhR>mcD8GFP vs *AkhR>EcR DN* | P0	<0.0001
drsl2	*AkhR>mcD8GFP* vs *AkhR>EcR DN* | L3	0.7280
	AkhR>mcD8GFP vs *AkhR>EcR DN* | P0	0.4609
drsl3	*AkhR>mcD8GFP* vs *AkhR>EcR DN* | L3	0.0001
	AkhR>mcD8GFP vs *AkhR>EcR DN* | P0	0.8518
drsl5	*AkhR>mcD8GFP* vs *AkhR>EcR DN* | L3	0.0058
	AkhR>mcD8GFP vs *AkhR>EcR DN* | P0	0.3890
Gene	**lsmeans, pairwise~Stage | Genotype**	**p-value**
cecropin A1	*AkhR>mcD8GFP* | L3 vs P0	<0.0001
	AkhR>EcR DN | L3 vs P0	0.0003
defensin	*AkhR>mcD8GFP* | L3 vs P0	<0.0001
	AkhR>EcR DN | L3 vs P0	<0.0001
metchnikowin	*AkhR>mcD8GFP* | L3 vs P0	<0.0001
	AkhR>EcR DN | L3 vs P0	0.3266
drs	*AkhR>mcD8GFP* | L3 vs P0	<0.0001
	AkhR>EcR DN | L3 vs P0	0.6709
drsl2	*AkhR>mcD8GFP* | L3 vs P0	<0.0001
	AkhR>EcR DN | L3 vs P0	<0.0001
drsl3	*AkhR>mcD8GFP* | L3 vs P0	<0.0001
	AkhR>EcR DN | L3 vs P0	0.0001
drsl5	*AkhR>mcD8GFP* | L3 vs P0	<0.0001
	AkhR>EcR DN | L3 vs P0	<0.0001

717

718 **S4 Table. Statistical analysis of AMP expression in samples with decreased ecdysone sensitivity in**
719 **the fat body (*AkhR>EcRDN*).** lsmeans, pairwise~Genotype | Stage represents differences within the
720 same stage, between genotypes. lsmeans, pairwise~Stage | Genotype represents the difference between
721 L3 and P0 within each genotype.

722

723

Gene	lsmeans, pairwise~Genotype | Stage	p-value
cecropin A1	*Mex>mcD8GFP* vs *Mex>EcR DN* | L3	0.0004
	Mex>mcD8GFP vs *Mex>EcR DN* | P0	<0.0001
defensin	*Mex>mcD8GFP* vs *Mex>EcR DN* | L3	0.7855
	Mex>mcD8GFP vs *Mex>EcR DN* | P0	<0.0001
metchnikowin	*Mex>mcD8GFP* vs *Mex>EcR DN* | L3	0.0371
	Mex>mcD8GFP vs *Mex>EcR DN* | P0	0.0060
drs	*Mex>mcD8GFP* vs *Mex>EcR DN* | L3	<0.0001
	Mex>mcD8GFP vs *Mex>EcR DN* | P0	0.0076
drsl2	*Mex>mcD8GFP* vs *Mex>EcR DN* | L3	0.8069
	Mex>mcD8GFP vs *Mex>EcR DN* | P0	<0.0001
drsl3	*Mex>mcD8GFP* vs *Mex>EcR DN* | L3	<0.0001
	Mex>mcD8GFP vs *Mex>EcR DN* | P0	0.0008
drsl5	*Mex>mcD8GFP* vs *Mex>EcR DN* | L3	0.9832
	Mex>mcD8GFP vs *Mex>EcR DN* | P0	0.4479
Gene	**lsmeans, pairwise~Stage | Genotype**	**p-value**
cecropin A1	*Mex>mcD8GFP* | L3 vs P0	0.0010
	Mex>EcR DN | L3 vs P0	0.0038
defensin	*Mex>mcD8GFP* | L3 vs P0	0.0028
	Mex>EcR DN | L3 vs P0	0.3866
metchnikowin	*Mex>mcD8GFP* | L3 vs P0	<0.0001
	Mex>EcR DN | L3 vs P0	<0.0001
drs	*Mex>mcD8GFP* | L3 vs P0	<0.0001
	Mex>EcR DN | L3 vs P0	<0.0001
drsl2	*Mex>mcD8GFP* | L3 vs P0	<0.0001
	Mex>EcR DN | L3 vs P0	<0.0001
drsl3	*Mex>mcD8GFP* | L3 vs P0	<0.0001
	Mex>EcR DN | L3 vs P0	0.2084
drsl5	*Mex>mcD8GFP* | L3 vs P0	<0.0001
	Mex>EcR DN | L3 vs P0	<0.0001

724

725 **S5 Table. Statistical analysis of AMP expression in samples with decreased ecdysone sensitivity in**
726 **the migut (*Mex>EcRDN*).** lsmeans, pairwise~Genotype | Stage represents differences within the same
727 stage, between genotypes. lsmeans, pairwise~Stage | Genotype represents the difference between L3
728 and P0 within each genotype.

729

730

Gene	lsmeans, pairwise~Genotype | Stage	p-value
cecropin A1	*Btl>mcD8GFP* vs *Btl>EcR DN* | L3	0.0197
	Btl>mcD8GFP vs *Btl>EcR DN* | P0	0.8417
defensin	*Btl>mcD8GFP* vs *Btl>EcR DN* | L3	0.1219
	Btl>mcD8GFP vs *Btl>EcR DN* | P0	0.0336
metchnikowin	*Btl>mcD8GFP* vs *Btl>EcR DN* | L3	<0.0001
	Btl>mcD8GFP vs *Btl>EcR DN* | P0	0.6789
drs	*Btl>mcD8GFP* vs *Btl>EcR DN* | L3	0.0098
	Btl>mcD8GFP vs *Btl>EcR DN* | P0	0.1636
drsl2	*Btl>mcD8GFP* vs *Btl>EcR DN* | L3	0.0197
	Btl>mcD8GFP vs *Btl>EcR DN* | P0	0.9116
drsl3	*Btl>mcD8GFP* vs *Btl>EcR DN* | L3	<0.0001
	Btl>mcD8GFP vs *Btl>EcR DN* | P0	0.4955
drsl5	*Btl>mcD8GFP* vs *Btl>EcR DN* | L3	0.4510
	Btl>mcD8GFP vs *Btl>EcR DN* | P0	0.1192
Gene	**lsmeans, pairwise~Stage | Genotype**	**p-value**
cecropin A1	*Btl>mcD8GFP* | L3 vs P0	<0.0001
	Btl>EcR DN | L3 vs P0	0.0001
defensin	*Btl>mcD8GFP* | L3 vs P0	0.0027
	Btl>EcR DN | L3 vs P0	0.0010
metchnikowin	*Btl>mcD8GFP* | L3 vs P0	<0.0001
	Btl>EcR DN | L3 vs P0	0.3711
drs	*Btl>mcD8GFP* | L3 vs P0	<0.0001
	Btl>EcR DN | L3 vs P0	<0.0001
drsl2	*Btl>mcD8GFP* | L3 vs P0	<0.0001
	Btl>EcR DN | L3 vs P0	<0.0001
drsl3	*Btl>mcD8GFP* | L3 vs P0	<0.0001
	Btl>EcR DN | L3 vs P0	0.0004
drsl5	*Btl>mcD8GFP* | L3 vs P0	<0.0001
	Btl>EcR DN | L3 vs P0	<0.0001

731

732 **S6 Table. Statistical analysis of AMP expression in samples with decreased ecdysone sensitivity in**
733 **the tracheal system (*btl>EcRDN*).** lsmeans, pairwise~Genotype | Stage represents differences within
734 the same stage, between genotypes. lsmeans, pairwise~Stage | Genotype represents the difference
735 between L3 and P0 within each genotype.

736

lsmeans, pairwise~Genotype | Stage	***p-value***
+;+;+ vs *+;+;Drs{w+}* | L3	0.9211
+;+;+ vs *+;+;Drs{w+}* | Pupa	0.2412
+;+;+ vs *+;+;Drs{w+}* | Adult	0.7340
lsmeans, pairwise~Stage | Genotype	***p-value***
+;+;+ | L3 vs Pupa	0.1774
+;+;+ | L3 vs Adult	0.7390
+;+;+ | Pupa vs Adult	1.0000
+;+;Drs{w+} | L3 vs Pupa	1.0000
+;+;Drs{w+} | L3 vs Adult	1.0000
+;+;Drs{w+} | Pupa vs Adult	1.0000

737

738 **S7 Table. Statistical analysis of mortality between genotypes, across stages**. lsmeans,

739 pairwise~Genotype | Stage represents differences within the same stage, between genotypes. lsmeans,

740 pairwise~Stage | Genotype represents the difference between L3 and P0 within each genotype.

741

742

Gene	**lsmeans, pairwise~Genotype | Stage**	**p-value**
cecropin A1	*Cg;Cas9>+;+;+* vs *Cg;Cas9>br KO* | L3	1.0000
	Cg;Cas9>+;+;+ vs *Cg;Cas9>br-Z4 KO* | L3	1.0000
	Cg;Cas9>br KO *Cg;Cas9>br-Z4 KO* | L3	1.0000
	Cg;Cas9>+;+;+ vs *Cg;Cas9>br KO* | P0	1.0000
	Cg;Cas9>+;+;+ vs *Cg;Cas9>br-Z4 KO* | P0	1.0000
	Cg;Cas9>br KO *Cg;Cas9>br-Z4 KO* | P0	1.0000
defensin	*Cg;Cas9>+;+;+* vs *Cg;Cas9>br KO* | L3	0.6537
	Cg;Cas9>+;+;+ vs *Cg;Cas9>br-Z4 KO* | L3	1.0000
	Cg;Cas9>br KO *Cg;Cas9>br-Z4 KO* | L3	0.5756
	Cg;Cas9>+;+;+ vs *Cg;Cas9>br KO* | P0	0.2314
	Cg;Cas9>+;+;+ vs *Cg;Cas9>br-Z4 KO* | P0	0.0003
	Cg;Cas9>br KO *Cg;Cas9>br-Z4 KO* | P0	0.0831
metchnikowin	*Cg;Cas9>+;+;+* vs *Cg;Cas9>br KO* | L3	1.0000
	Cg;Cas9>+;+;+ vs *Cg;Cas9>br-Z4 KO* | L3	1.0000
	Cg;Cas9>br KO *Cg;Cas9>br-Z4 KO* | L3	0.7209
	Cg;Cas9>+;+;+ vs *Cg;Cas9>br KO* | P0	0.8651
	Cg;Cas9>+;+;+ vs *Cg;Cas9>br-Z4 KO* | P0	1.0000
	Cg;Cas9>br KO *Cg;Cas9>br-Z4 KO* | P0	0.4444

drs	*Cg;Cas9>+;+;+* vs *Cg;Cas9>br KO* | L3	1.0000
	Cg;Cas9>+;+;+ vs *Cg;Cas9>br-Z4 KO* | L3	1.0000
	Cg;Cas9>br KO *Cg;Cas9>br-Z4 KO* | L3	1.0000
	Cg;Cas9>+;+;+ vs *Cg;Cas9>br KO* | P0	<0.0001
	Cg;Cas9>+;+;+ vs *Cg;Cas9>br-Z4 KO* | P0	<0.0001
	Cg;Cas9>br KO *Cg;Cas9>br-Z4 KO* | P0	0.0002
drsl2	*Cg;Cas9>+;+;+* vs *Cg;Cas9>br KO* | L3	1.0000
	Cg;Cas9>+;+;+ vs *Cg;Cas9>br-Z4 KO* | L3	1.0000
	Cg;Cas9>br KO *Cg;Cas9>br-Z4 KO* | L3	1.0000
	Cg;Cas9>+;+;+ vs *Cg;Cas9>br KO* | P0	1.0000
	Cg;Cas9>+;+;+ vs *Cg;Cas9>br-Z4 KO* | P0	1.0000
	Cg;Cas9>br KO *Cg;Cas9>br-Z4 KO* | P0	1.0000
drsl3	*Cg;Cas9>+;+;+* vs *Cg;Cas9>br KO* | L3	1.0000
	Cg;Cas9>+;+;+ vs *Cg;Cas9>br-Z4 KO* | L3	1.0000
	Cg;Cas9>br KO *Cg;Cas9>br-Z4 KO* | L3	1.0000
	Cg;Cas9>+;+;+ vs *Cg;Cas9>br KO* | P0	1.0000
	Cg;Cas9>+;+;+ vs *Cg;Cas9>br-Z4 KO* | P0	0.9050
	Cg;Cas9>br KO *Cg;Cas9>br-Z4 KO* | P0	0.9168
drsl5	*Cg;Cas9>+;+;+* vs *Cg;Cas9>br KO* | L3	0.9520
	Cg;Cas9>+;+;+ vs *Cg;Cas9>br-Z4 KO* | L3	0.0167
	Cg;Cas9>br KO *Cg;Cas9>br-Z4 KO* | L3	0.2020
	Cg;Cas9>+;+;+ vs *Cg;Cas9>br KO* | P0	0.1613
	Cg;Cas9>+;+;+ vs *Cg;Cas9>br-Z4 KO* | P0	0.3062
	Cg;Cas9>+;+;+ *Cg;Cas9>br-Z4 KO* | P0	1.0000
Gene	**lsmeans, pairwise~Stage | Genotype**	**p-value**
cecropin A1	*Cg;Cas9>+;+;+* | L3 vs P0	<0.0001
	Cg;Cas9>br KO | L3 vs P0	<0.0001
	Cg;Cas9>br-Z4 KO | L3 vs P0	<0.0001
defensin	*Cg;Cas9>+;+;+* | L3 vs P0	<0.0001
	Cg;Cas9>br KO | L3 vs P0	<0.0001
	Cg;Cas9>br-Z4 KO | L3 vs P0	<0.0001
metchnikowin	*Cg;Cas9>+;+;+* | L3 vs P0	<0.0001
	Cg;Cas9>br KO | L3 vs P0	<0.0001
	Cg;Cas9>br-Z4 KO | L3 vs P0	<0.0001
drs	*Cg;Cas9>+;+;+* | L3 vs P0	<0.0001
	Cg;Cas9>br KO | L3 vs P0	0.0001
	Cg;Cas9>br-Z4 KO | L3 vs P0	0.4691

drsl2	*Cg;Cas9>+;+;+* | L3 vs P0	<0.0001
	Cg;Cas9>br KO | L3 vs P0	<0.0001
	Cg;Cas9>br-Z4 KO | L3 vs P0	<0.0001
drsl3	*Cg;Cas9>+;+;+* | L3 vs P0	<0.0001
	Cg;Cas9>br KO | L3 vs P0	<0.0001
	Cg;Cas9>br-Z4 KO | L3 vs P0	<0.0001
drsl5	*Cg;Cas9>+;+;+* | L3 vs P0	<0.0001
	Cg;Cas9>br KO | L3 vs P0	<0.0001
	Cg;Cas9>br-Z4 KO | L3 vs P0	<0.0001

743

744 **S8 Table. Statistical analysis of AMP expression when *br* or *br-Z4* are knocked-out specifically in**
745 **the fat body and haemocytes.** lsmeans, pairwise~Genotype | Stage represents differences within the
746 same stage, between genotypes. L3 is coloured in red and P0 in blue. lsmeans, pairwise~Stage |
747 Genotype represents the difference between L3 and P0 within each genotype. Different shades
748 represent different genotypes

Primer name	***5'-Sequence-3' (Capital: gRNA sequences)***
br_common_PCR1_F01	cggcccgggttcgattcccggccgatgcaGGGGAGTTGGCAATATAGAGgtttcagagctatgctggaaac
br_common_PCR1_R01	TGGGCTCACCAATGCCAATCtgcaccagccgggaatcgaacc
br_common_PCR2_F01	GATTGGCATTGGTGAGCCCAgtttcagagctatgctggaaac
br_common_PCR2_R01	GCGAGGTGTGCGGTGCGACCtgcaccagccgggaatcgaacc
br_common_PCR3_F01	GGTCGCACCGCACACCTCGCgtttcagagctatgctggaaac
br_common_PCR3_R01	attttaacttgctatttctagctctaaaacCTGCCCACACATGACGTGTCtgcaccagccgggaatcgaacc
br_Z4_PCR1_F01	cggcccgggttcgattcccggccgatgcaGGAATTTATCTGGCTCTCATgtttcagagctatgctggaaac
br_Z4_PCR1_R01	CAACAACTAGACATGAACGCtgcaccagccgggaatcgaacc
br_Z4_PCR2_F01	GCGTTCATGTCTAGTTGTTGgtttcagagctatgctggaaac
br_Z4_PCR2_R01	CCTCCCGATCCACCCGCCGCtgcaccagccgggaatcgaacc
br_Z4_PCR3_F01	GCGGCGGGTGGATCGGGAGGgtttcagagctatgctggaaac
br_Z4_PCR3_R01	attttaacttgctatttctagctctaaaacCCGTACTCCTGTCCGCCTCCtgcaccagccgggaatcgaacc

749

750 **S9 Table. 5'-3' sequences of primers used for tissue specific CRISPR.** Guide RNA (gRNA)
751 sequences are represented in capital letters.

Primer name	***5'-Sequence-3'***
rpl32 F01	CCAGTCGGATCGATATGCTAA
rpl32 R01	GTTCGATCCGTSACCGATGT
dif F01	CACAGTGGGCAACTCAAAAGTG
dif R01	GATGTCGTCCTTGGCAATCTTC
relish F01	ACAAAGGACGAGGATTCCGTGG
relish R01	TGATTCAGCAGCGAACAGAGCC
drosomycin F01	CTCTTCGCTGTCCTGATGCTGG
drosomycin R01	GACAGGTCTCGTTGTCCCAGAC
diptericin F01	TACTTTGGCTTATCCGATGCCC
diptericin R01	GTGCTGTCCATATCCTCCATTC
cecropin a1 F01	GTTTTCGTCGCTCTCATTCTGG
cecropin a1 R01	CTTGTTGAGCGATTCCCAGTC
defensin F01	TCGCTTTTGCTCTGCTTGCTTG
defensin R01	GTTGCAGTAGCCGCCTTTGAAC
metchnikowin F01	AGCGATTTTTCTGGCCCTGCTGG
metchnikowin R01	CTTGGTTGGTTAGGATTGAAGG
drsl2 F01	CCTGGCTGTGATGACAATTGTTG
drsl2 R01	ACTGATATGTCCCTCCTCCTTGC
drsl3 F01	TCCTAATGGAGGCCAACACTG
drsl3 R01	TCCCTCCTCAATGCAGAGACG
drsl5 F01	TCCTGGCTGTGATGACCATCTTC
drsl5 R01	ACTGGATCGTCCTTCCTCCTTG
br F01	CAATGCCAACGACGAACACAGCAA
br R01	ATTGGGAAAGTTGAAGGCGGCTG
Br-Z4 F01	GAACCACCACTCGTATTTCCAC
bR-Z4 R01	ACCGCCCACATTAACGCTATTG

752

753 **S10 Table. 5'-3' sequences of primers used for qPCR**